



Maxwell's Equations and Electromagnetics after 150 Years

Weng Cho Chew^{1,2}

Lijun Jiang²; Sheng Sun²; Wei E.I. Sha²; Q. I. Dai¹; Yan Lin Li²; Qin Liu²;
Tian Xia¹, Hui Gan¹, Mike Wei¹, Ai Yin Liu¹; Christopher Ryu¹; Shu Chen¹

¹University of Illinois, USA, ²The University of Hong Kong

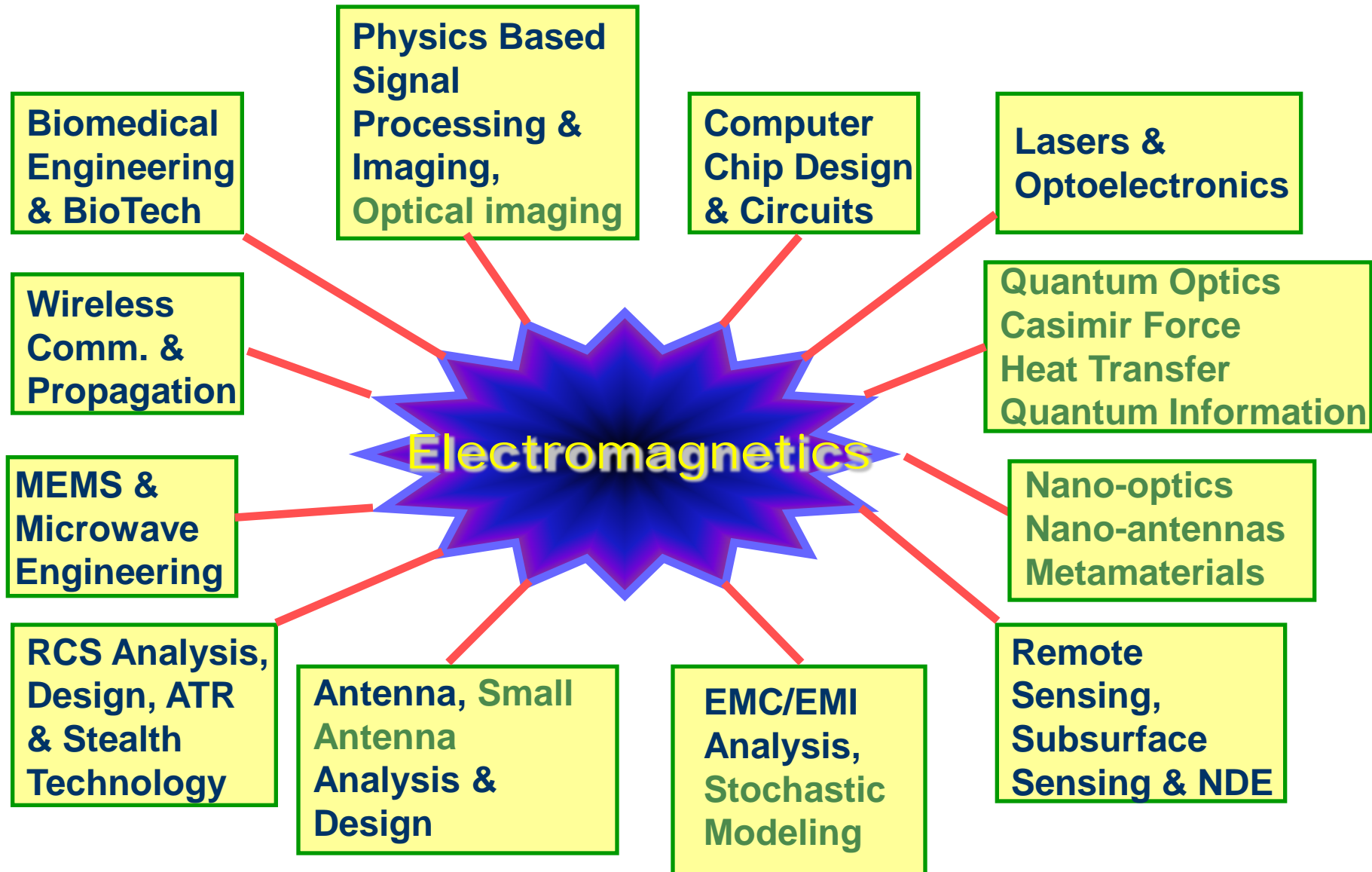
ECE Distinguished Seminar
Purdue University
March 9, 2016

Maxwell's Equations (Not in Comatose!)

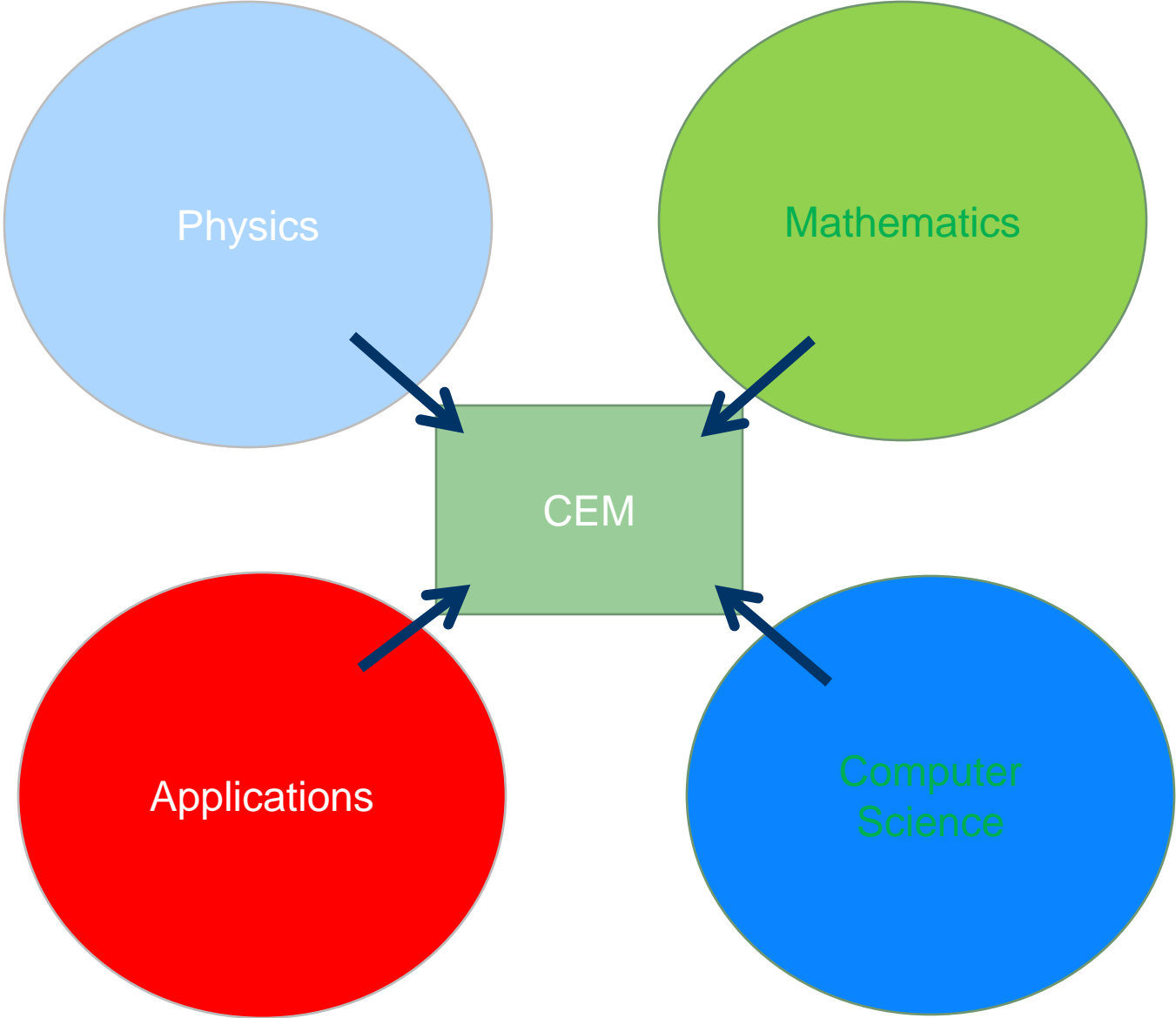
- Valid over a vast length scale and broad frequency range.
 - **From subatomic dimension to galactic dimension; static to ultra-violet.**
- Relativistic invariance (special relativity, Einstein, 1905).
 - **Equations remain the same in all inertial frame.**
- Valid in the quantum regime as well (Dirac, 1927).
 - **Dyadic Green's function is still needed in quantum regime.**
 - **Coherent state in quantum optics by Glauber, 1968. (2005 Nobel Laureate)**
- In harmony with differential geometry (Cartan, 1945)
 - **Differential forms and Yang-Mills theory (1954). Differential forms illuminate EM theory, and EM theory illuminates differential forms (quote from Misner, Thorne, and Wheeler).**
- One of the most accurate equations (Feynman, 1985, Aoyama et al, Styer, 2012).
 - **Validated to a few parts in a trillion.**
- Tremendous impact in science and technology.
 - **Electrical engineering, optics, wireless and optical communications, computers, remote sensing, bioelectromagnetics, etc.**

Importance of Electromagnetics and its Enduring Legacy

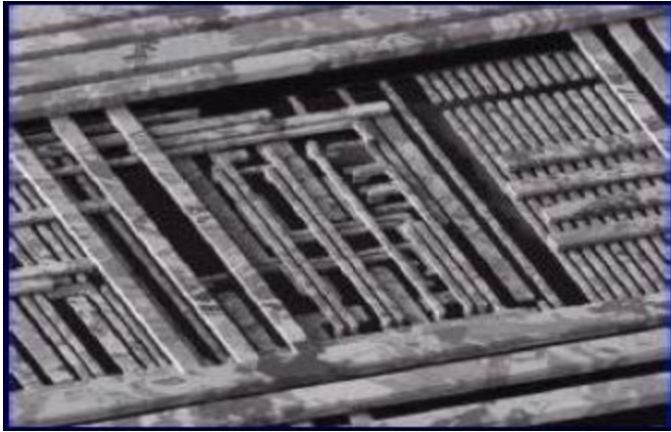
--20+ years Later



Areas Driving and Inspiring Computational Electromagnetics (CEM)



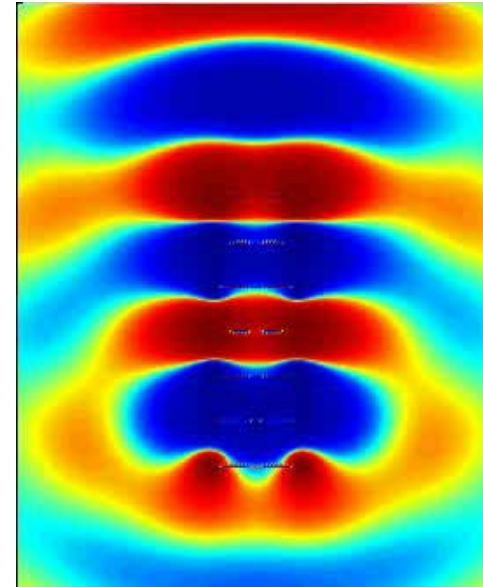
Intro: The Tale of Three Physics; Circuit Physics; Wave Physics; Ray Physics; (not to mention quantum physics)



Circuit Physics



Wave Physics

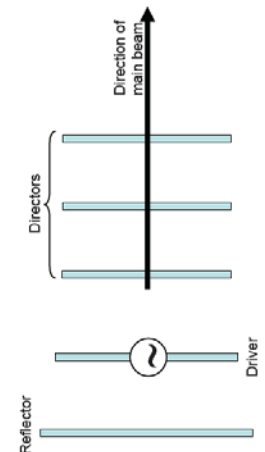
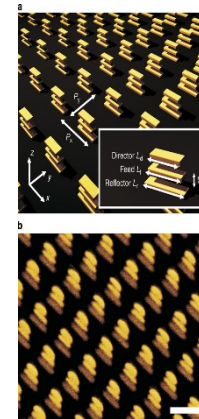


Yagi-Uda 1926

Inspired nano-antennas:
Dragely et al.



Ray Physics



A Brief History of Electromagnetics and Optics

- Lode stone 400BC, Compass 200BC
- Static electricity, Greek, 400 BC
- Ampere's Law 1823;
- Faraday Law 1838;
- KCL/KVL 1845
- Telegraphy (Morse) 1837;
- Electrical machinery (Sturgeon) 1832;
 - Maxwell's equations 1864/1865;
 - Heaviside, Hertz, Rayleigh, Sommerfeld, Debye, Mie, Kirchhoff, Love, Lorentz (plus many unsung heroes);
 - Quantum electrodynamics 1927 (Dirac, Feynman, Schwinger, Tomonaga);
 - Electromagnetic technology;
- Nano-fabrication technology;
- Single-photon measurement;
- Quantum optics/Nano-optics 1980s;
- Quantum information/Bell's theorem 1980s;
- Quantum electromagnetics/optics (coming).
- Pinhole camera, 400BC, Mozi,
- Ibn Sahl, refraction 984;
- Snell, 1621;
- Huygens/Newton 1660;
- Fresnel 1814;
- Kirchhoff 1883;

Electromagnetics (EM) /Optics Technologies

Electromagnetics

- Antennas;
 - **Communications;**
- Radars;
- Maser (1952);
- Remote sensing;
- Synthetic Aperture Radar;
- Interferometric radar;
- Computational electromagnetics;

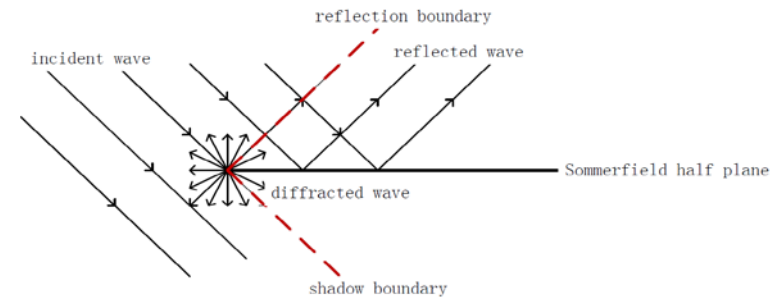
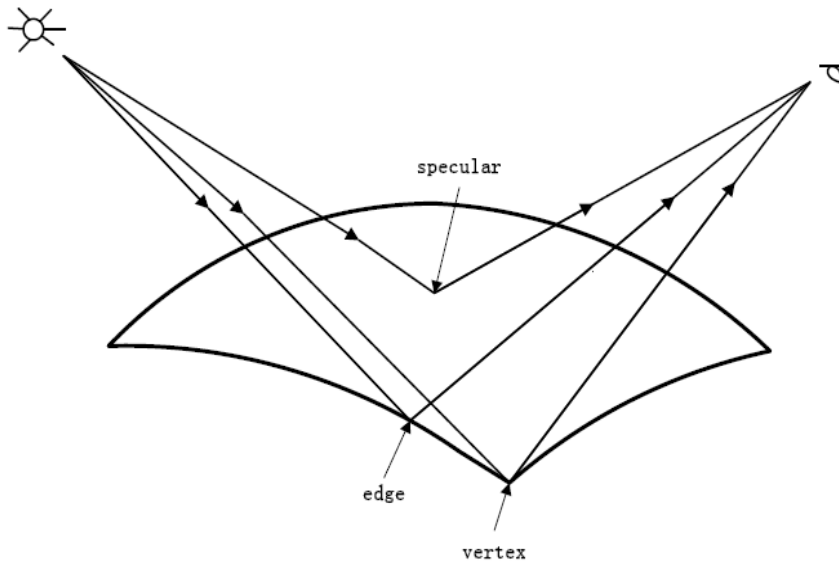
Optics

- Lens;
- Lasers (1958);
- Semiconductor lasers ($h\omega$);
- LEDs;
- Opto-electronics;
- Interferometric imaging;
 - **Optical Coherence Tomography;**
 - **Optical phase imaging;**
- Nano-optics;
 - **Nano-antennas.**

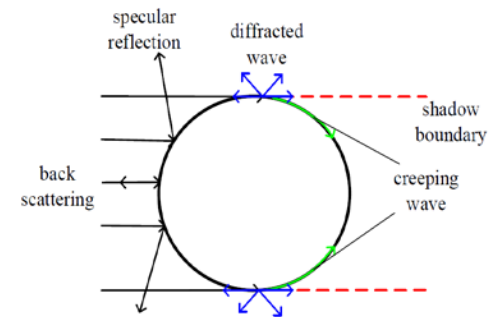
Age of Approximations

- High Frequency Asymptotics (Ray Physics);

Sommerfeld Half Plane



Cylinder Scattering: Watson Transformation



J. B. Keller, *JOSA*, vol. 52, pp.116–130, 1962.

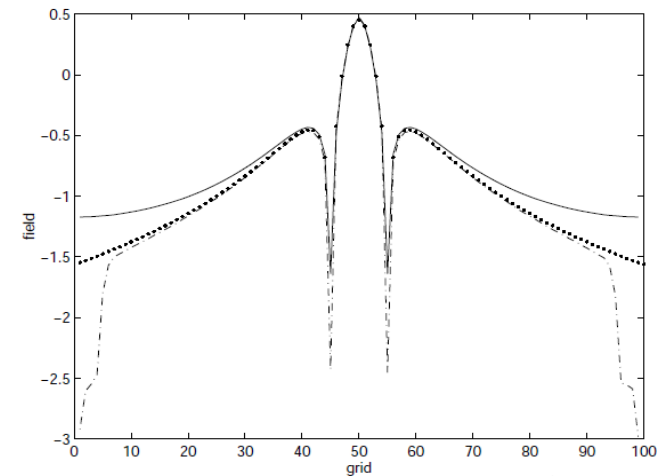
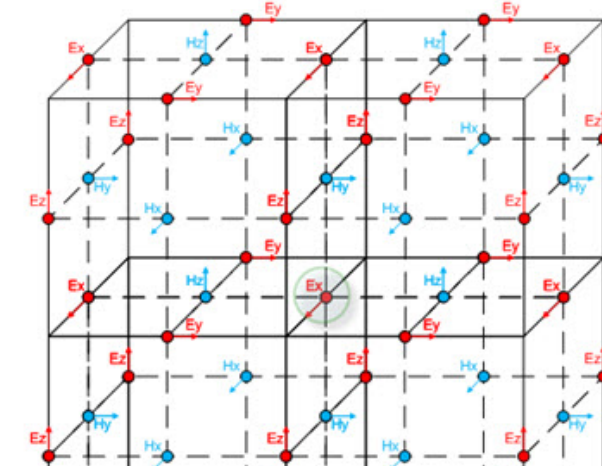
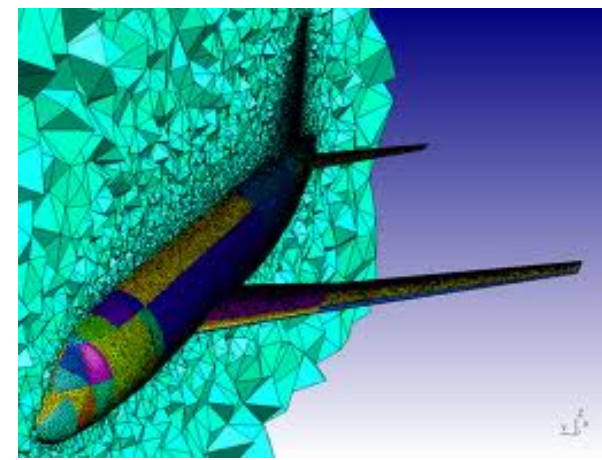
R. G. Kouyoumjian and P. H. Pathak *Proc. IEEE*, vol. 62, pp. 1448–1461, 1974.

S.W. Lee and G.A. Deschamps, *Antennas and Propagation, IEEE Transactions on*, 24.1: 25-34, 1976.

P. Y. Ufimtsev, *Fundamentals of the physical theory of diffraction*, New York: John Wiley and Sons, Inc., 2007.

Age of Computations

- Galerkin, 1915; subspace projection.
- Finite element methods; Silvester & Ferrari, Mei, Cendes & Lee, Volakis, Jin etc (1960s-1980s).
- Differential forms and differential geometry (Cartan, 1945; Deschamps; Desbrun);
 - **One forms, E, H , are curl conforming;**
 - **Two forms, B, D , are divergence conforming;**
- Yee grid (1960s) fits with differential forms easily;
 - **Staggered grids and dual grids;**
 - **Coordinate stretching Perfectly Matched Layer;**
 - **Works even for static field;**
- Allen Taflove; FDTD (1990s);
- Berenger; PML, Sacks, Lee & Lee etc (1990s)
- Coordinate Stretching PML Chew Weedon (1994);



W.C. Chew, W.H. Weedon and A. Sezginer, Proc.

11th ACES, pp. 482-489, March 20-25, 1995.

Integral Equation Method (Moment of Moments History)

- Kravchuk, 1932;
 - Kantorovich, Krylov
- Harrington 1967;
- Richmond 1965;
- Numerical Electromagnetics Code,
 - Burke, Poggio, Logan, Rockway, 1977.
 - Miller
- Rao-Wilton-Glisson patch basis, 1982;

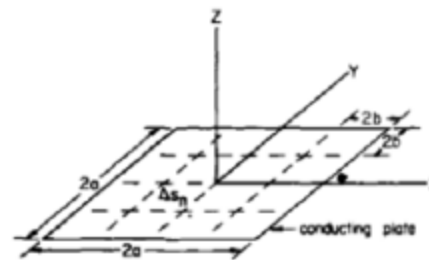


Fig. 1. A square conducting plate.

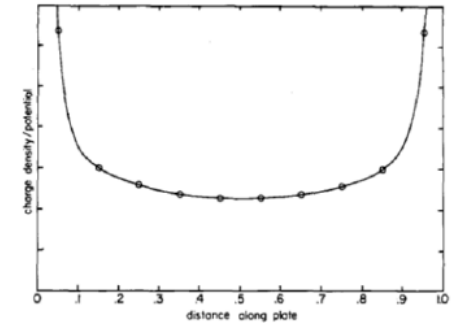
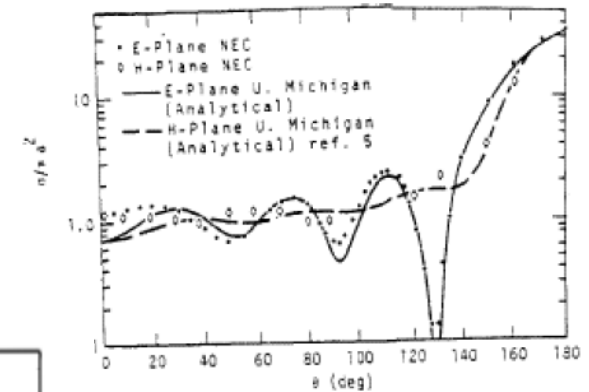


Fig. 2. Approximate charge density on subareas closest to the centerline of a square plate.



(a) Uniform Segmentation

4. Bistatic RCS of a Sphere with $ka = 5.3$.

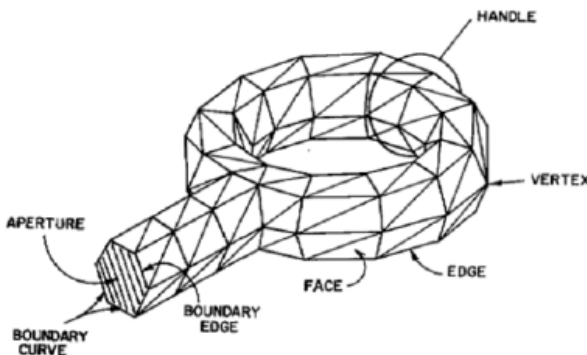


Fig. 1. Arbitrary surface modeled by triangular patches.

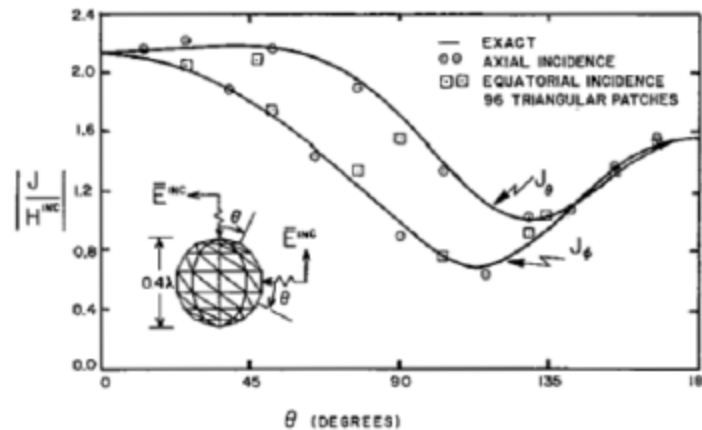


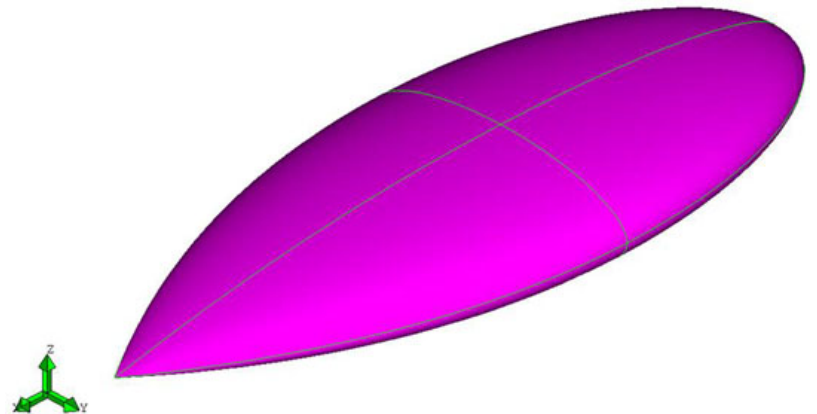
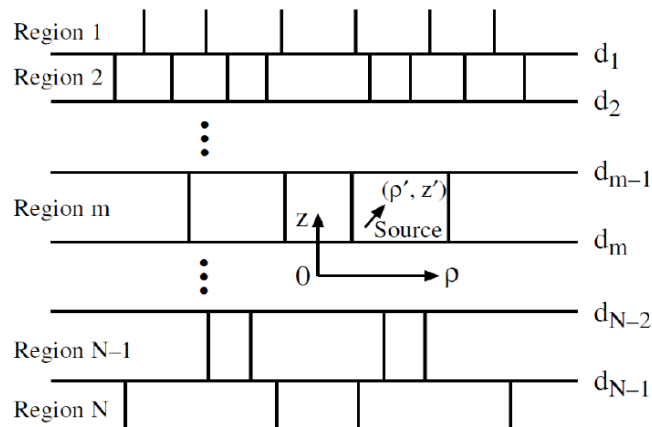
Fig. 10. Distribution of current components on 0.2λ radius conducting sphere.

Age of Computation--Early Days

- In the early days, only several thousand unknowns are possible on a workstation using MoM or integral equation solvers;
- Tens of thousands of unknowns are possible using FDTD on a workstation;
- So FDTD was far ahead of MoM in popularity in the late 1980s;
- In the 80s, mode matching methods were developed;
- However, in the early 1990s, fast algorithms for integral equations started to emerge;
- They use a divide and defeat (DaD) scheme.

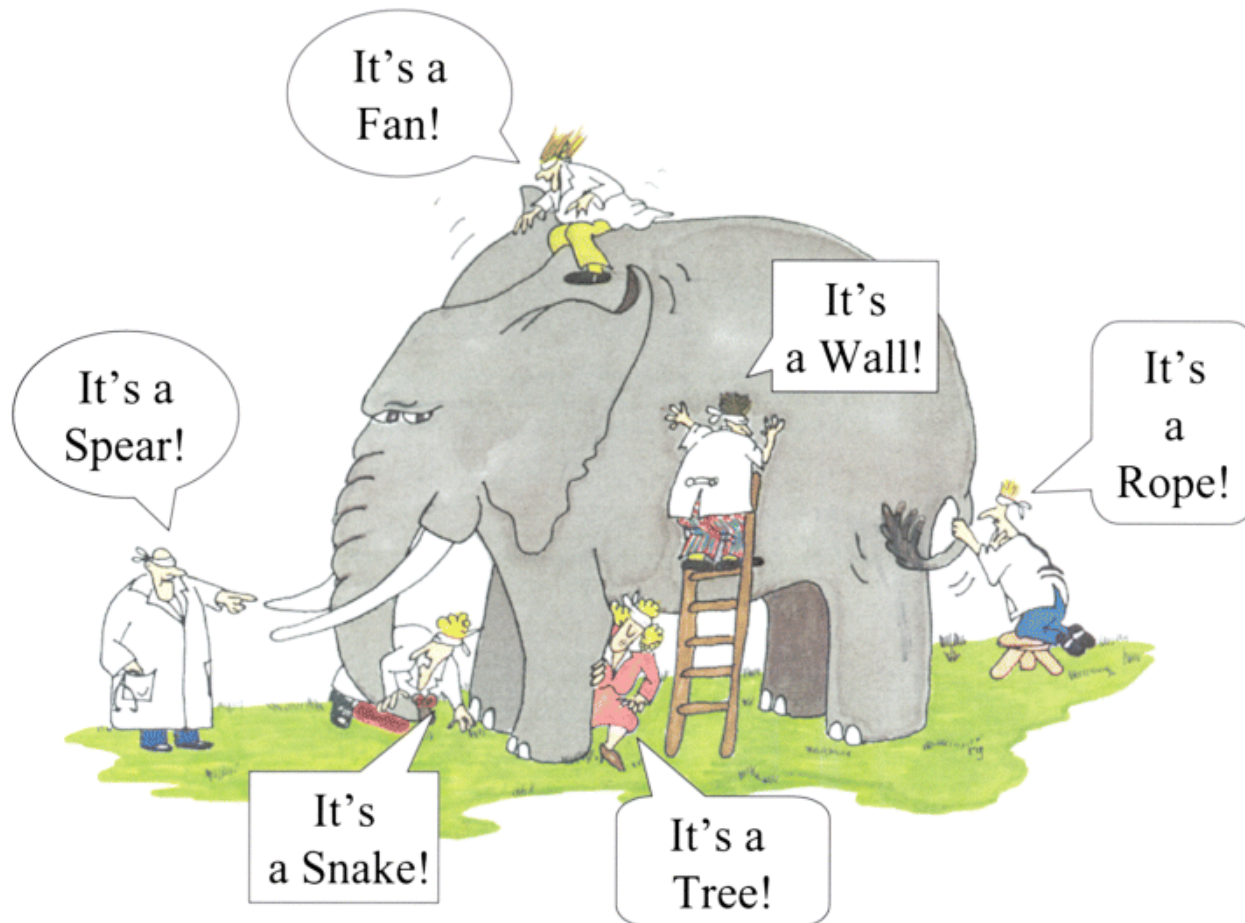
Fast Algorithms Needed

- Curse of dimensionality; $N = Ck^{4.5}$
 - Unknown count grows rapidly with frequency in 3D.
 - RCWA (Rigorous Coupled Mode Analysis), Moharam and Gaylord, 1981.
 - Semi-analytic numerical mode-matching method, 1984. Chew et al.
 - Replace FEM, FDM, and VIE with surface integral equations.



Famous Indian Proverb

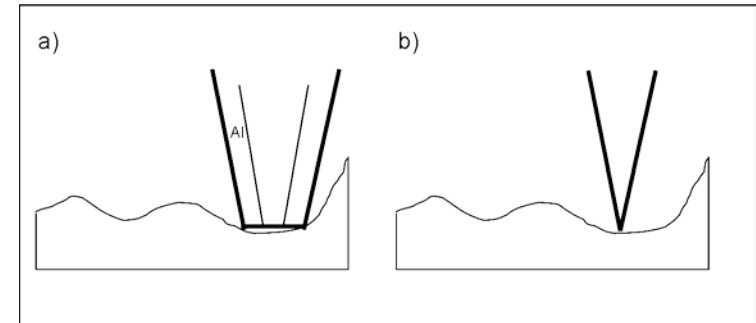
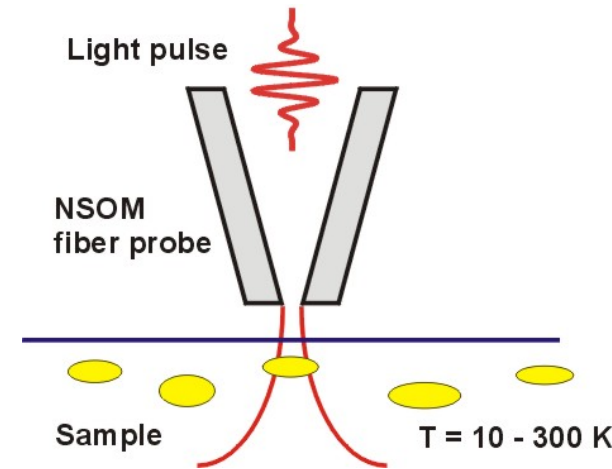
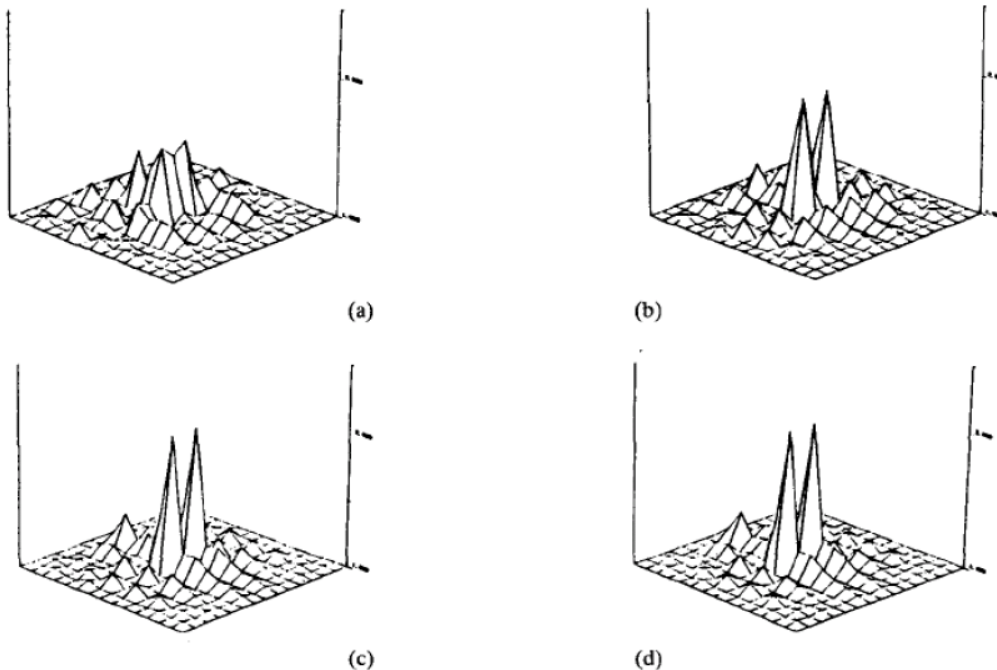
- What's in the history of CEM, one man can't tell all!



Fast Algorithms--Contd

- Cruelty of computational complexity;
 - In the beginning, developed fast algorithm to address the inverse scattering problem;
 - Super-resolution inverse problem—Distorted Born Iterative Method (DBIM)

Evanescent waves needed for super-resolution



Super-resolution Inversion

- With W.H. Weedon, F.C. Chen, P.E. Mayes

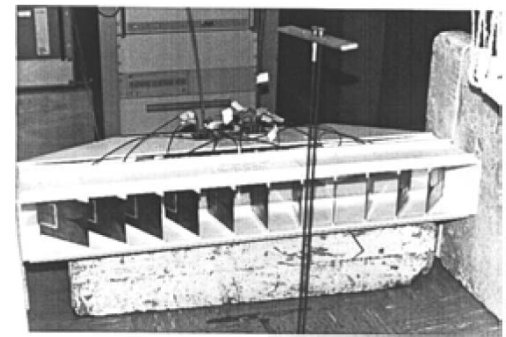


Figure 5. Photograph of broadband switched antenna array containing 11 identical broadband Vivaldi antennas and two microwave switches enclosed in a polystyrene housing.

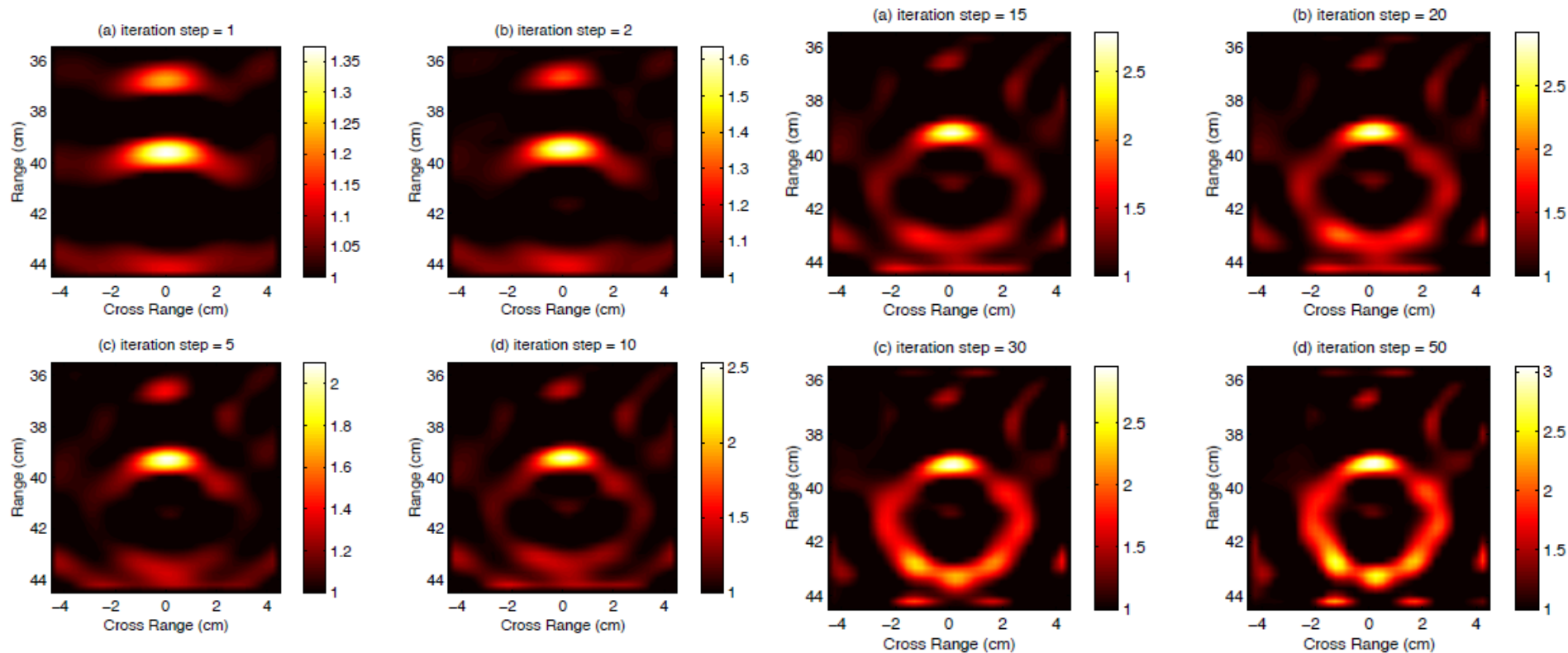


Figure 3.6 DBIM permittivity reconstruction image of a hollow plastic pipe. (4.8 cm in outer diameter, 3.7 cm in inner diameter) at different iteration steps. (a) Iteration step = 1, (b) iteration step = 2, (c) iteration step = 5, and (d) iteration step = 10.

Figure 3.7 DBIM permittivity reconstruction image of a hollow plastic pipe. (4.8 cm in outer diameter, 3.7 cm in inner diameter) at different iteration steps. (a) Iteration step = 15, (b) iteration step = 20, (c) iteration step = 30, and (d) iteration step = 50.

Recursive Algorithms

L. Gürel and W. C. Chew, "A recursive T-matrix algorithm for strips and patches," Radio Science, vol. 27, no. 3, pp. 387-401, May-June 1992.

- Use the n -unknown problem to solve the $(n+1)$ -unknown problem;

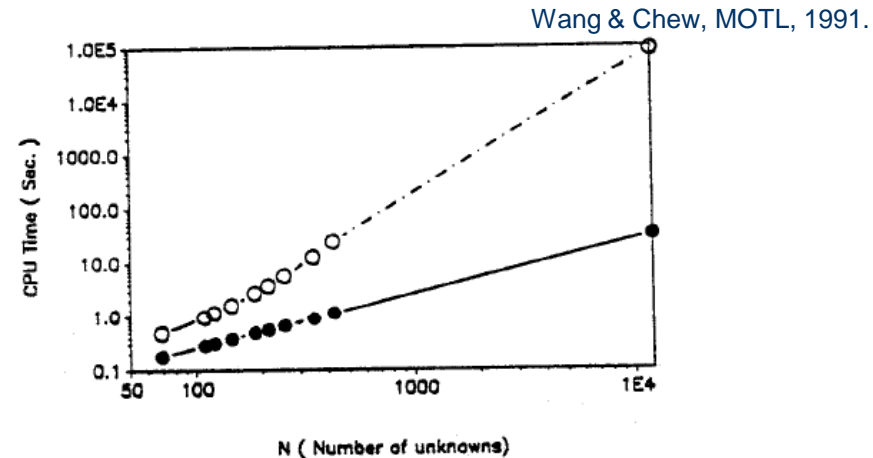


Figure 2 Comparison of the computer time as a function of the number of unknowns for the method of moment (open circles) and fast recursive algorithm (solid circles). At 12,000 unknown, the method of moments is estimated to take 20 h of CRAY-2 cpu time, while the fast recursive algorithm takes only 30 s of CRAY-2 cpu time to solve the same problem

- Recursive aggregate T matrix algorithm (RATMA);
- Computational complexity is $O(N^2)$ in 2D and $O(N^{2.33})$ in 3D for multiple right-hand side;
- Memory usage is $O(N)$ in 2D and $O(N^{1.33})$ in 3D.

Nested Equivalence Principle Algorithm (NEPAL)

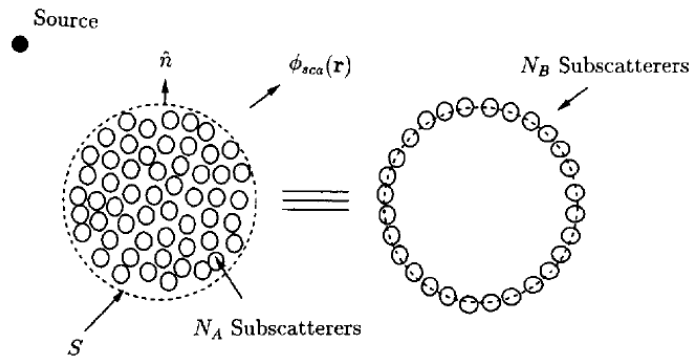


Fig. 1. Huygens' equivalence principle is used to replace the volume scattering centers by surface scattering centers.

W. C. Chew and C. C. Lu, "NEPAL--An algorithm for solving the volume integral equation," *Micro. Opt. Tech. Letters*, vol. 6, no. 3, pp. 185-188, Mar. 1993.

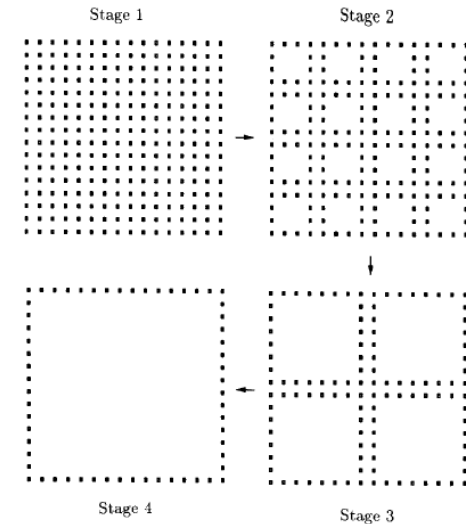
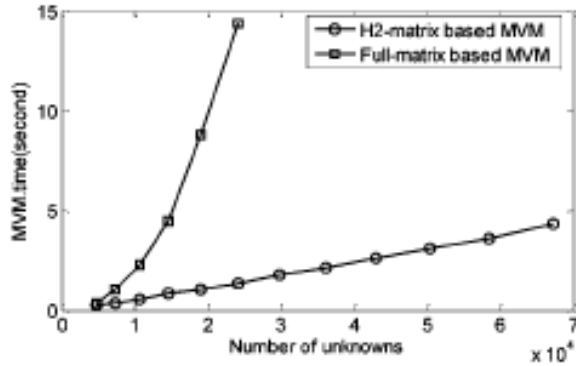


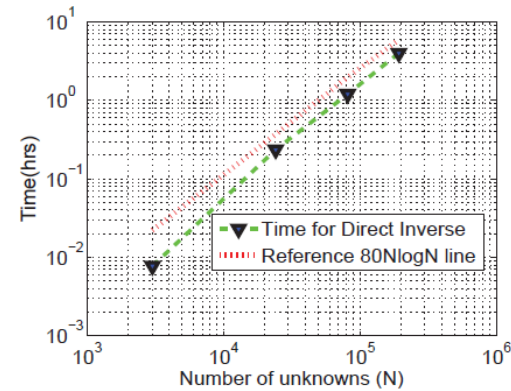
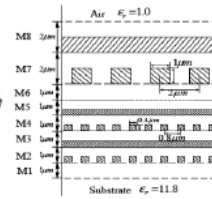
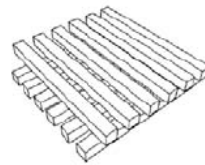
Fig. 2. By nesting a smaller problem within a larger one, Huygens' equivalence principle is used to reduce gradually the number of scattering centers by surface scattering centers. Scattering problems are also solved at each stage.

- Volume scatterers are replaced by surface scatterers;
- By recursively nesting smaller problems within larger problems, the volume scattering problem can be solved rapidly;
- Computational complexity is $O(N^{1.5})$ in 2D and $O(N^2)$ in 3D for wave physics;
- Memory usage is $O(N)$ in 2D and $O(N^{1.33})$ in 3D.

Fast Direct Solvers of Dan Jiao's Group



With W.W. Chai



(c) Scaling of inversion time.

With O. Saad

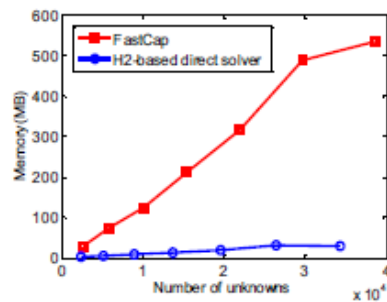
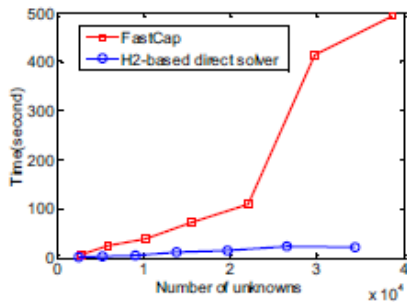
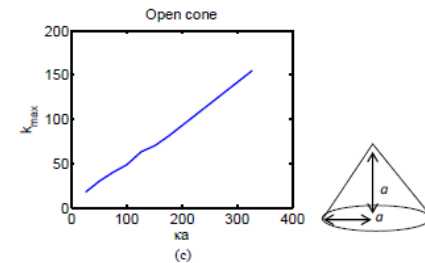
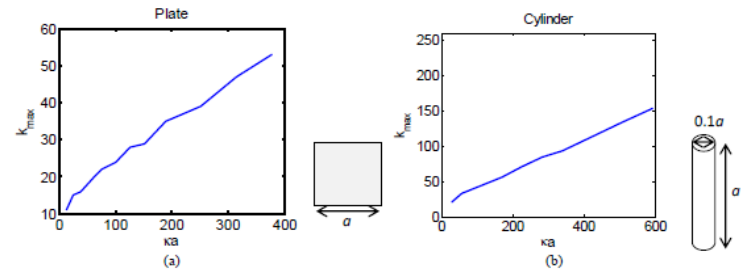


Fig. 6. Comparison of time and memory complexity in simulating the bus structure in free space.

With W.W. Chai

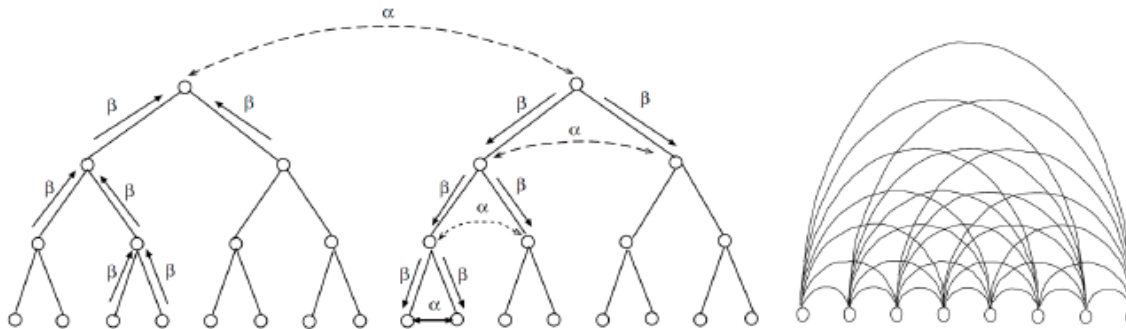


Rank of matrices

Fast Algorithms--Contd

- Curbing the cruelty of computational complexity;
- FFT based methods;
 - **AIMS, PC-FFT, CG-FFT, G-FFT, IE-FFT, FMM-FFT ($N^{1.5} \log N$ for surface scatterers)**
- FMM—Rokhlin, Greengard, Wandzura, Appel, Barnes, Hut
- Factorization of matrix elements (MLFMA); $N \log N$ for surface scatterers and electrodynamics;

$$L_{ij} = \tilde{\mathbf{V}}_{f,i,i_1}^t \cdot \bar{\mathbf{I}}_1 \cdot \tilde{\boldsymbol{\beta}}_{i_1,i_2} \cdot \bar{\mathbf{I}}_2 \cdots \tilde{\boldsymbol{\beta}}_{i_N,L} \cdot \tilde{\boldsymbol{\alpha}}_{LL'} \cdot \tilde{\boldsymbol{\beta}}_{L',j_N} \cdots \bar{\mathbf{I}}_2 \cdot \tilde{\boldsymbol{\beta}}_{j_2,j_1} \cdot \bar{\mathbf{I}}_1 \cdot \tilde{\mathbf{V}}_{s,j_1,j}$$



Smooth vs Oscillatory Green's Function (Kernel)

Circuit Physics

- Higher order derivatives become smaller and smaller:

$$G(\mathbf{r}, \mathbf{r}') = \frac{1}{4\pi|\mathbf{r} - \mathbf{r}'|}.$$

$$\frac{\partial}{\partial x} \frac{1}{|x|} = -\frac{1}{|x|^2} \rightarrow 0, \quad O\left(\frac{1}{x^2}\right), \quad x \rightarrow \infty$$

$$\frac{\partial^2}{\partial x^2} \frac{1}{|x|} = -\frac{\partial}{\partial x} \frac{1}{|x|^2} = \frac{2}{|x|^3} \rightarrow O\left(\frac{1}{x^3}\right), \quad x \rightarrow \infty$$

$$\frac{\partial^3}{\partial x^3} \frac{1}{|x|} = \frac{\partial}{\partial x} \frac{2}{|x|^3} = -\frac{6}{|x|^4} \rightarrow O\left(\frac{1}{x^4}\right), \quad x \rightarrow \infty$$

Wave Physics

- Higher order derivatives do not become smaller and smaller:**

$$G(\mathbf{r}, \mathbf{r}') = \frac{e^{ik_0|\mathbf{r} - \mathbf{r}'|}}{4\pi|\mathbf{r} - \mathbf{r}'|}.$$

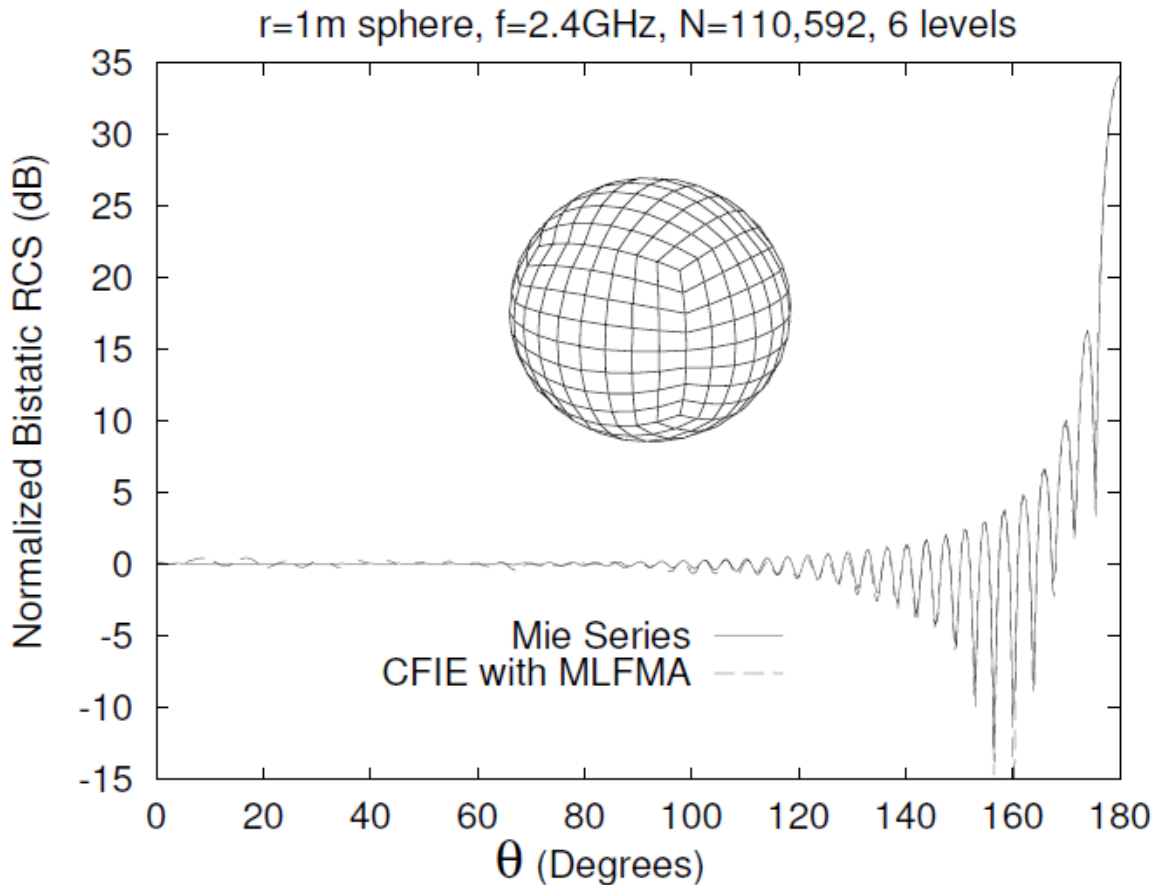
$$\frac{\partial}{\partial x} \frac{e^{ik|x|}}{|x|} = -\frac{e^{ik|x|}}{|x|^2} + ik \frac{e^{ik|x|}}{|x|} \rightarrow O\left(\frac{1}{x}\right), \quad x \rightarrow \infty$$

$$\frac{\partial^2}{\partial x^2} \frac{e^{ik|x|}}{|x|} \sim -k^2 \frac{e^{ik|x|}}{|x|} + H.O.T. \rightarrow O\left(\frac{1}{x}\right), \quad x \rightarrow \infty$$

$$\frac{\partial^3}{\partial x^3} \frac{e^{ik|x|}}{|x|} \sim -ik^3 \frac{e^{ik|x|}}{|x|} + H.O.T. \rightarrow O\left(\frac{1}{x}\right), \quad x \rightarrow \infty$$

The First Result that Shock the Community

- Dense matrix system for surface scatterer with 110,000 unknowns solved with MLFMA.

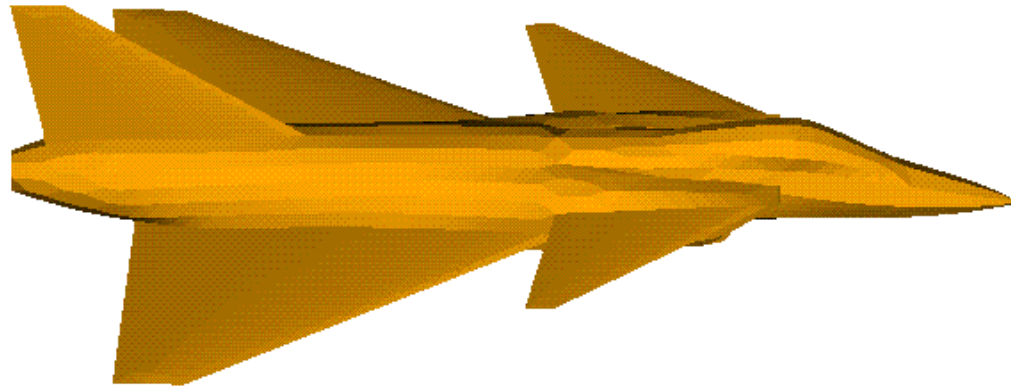


J. M. Song and W. C. Chew, "Multilevel fast-multipole algorithm for solving combined field integral equations of electromagnetic scattering," *Mico. Opt. Tech. Lett.*, vol. 10, no. 1, pp 14-19, Sept. 1995.

Use 300 MB of memory
on a single CPU SUN SPARC 10.

VFY218 at 8 GHz

1999, FISC (w/ JM Song, CC Lu, SW Lee)



	Nodes	Facets	Unknowns
Original	2,844	5,684	8,526
8 GHz	3,330,308	6,660,612	9,990,918

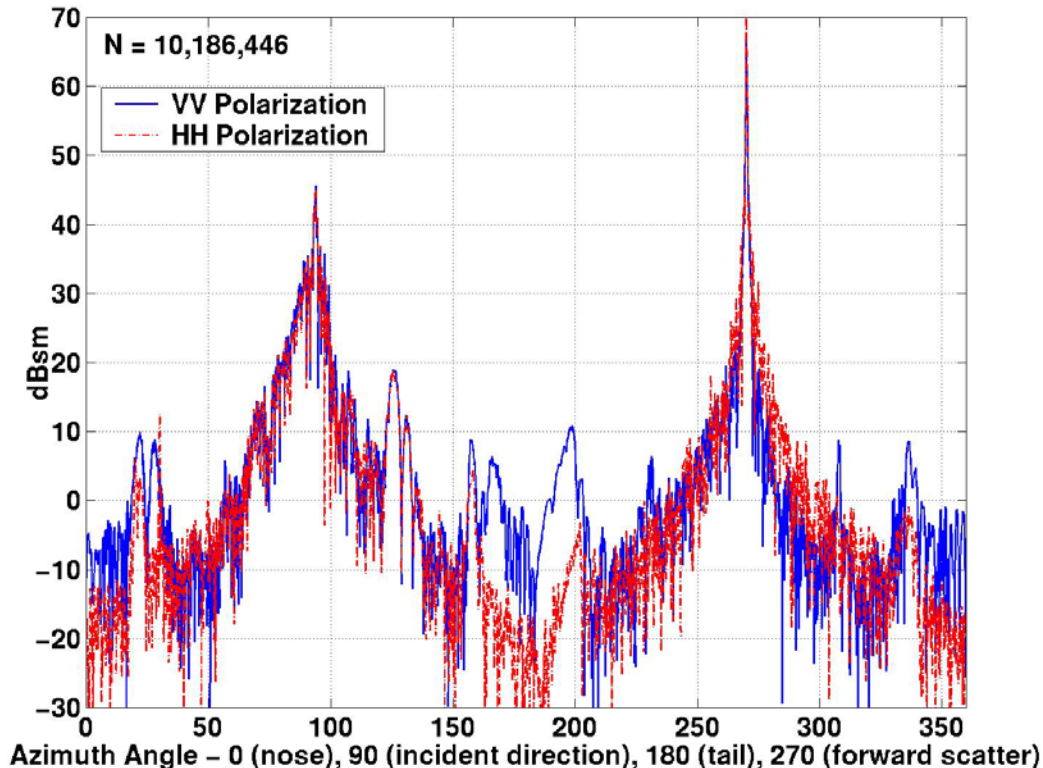
	Length	Width	Height
Inch	609"	350"	161"
8 GHz	412λ	237λ	109λ

The longest edge is 0.3λ , the average is 0.2λ , and
the surface area is $115,789 \lambda^2$
10-level MLFMA is used

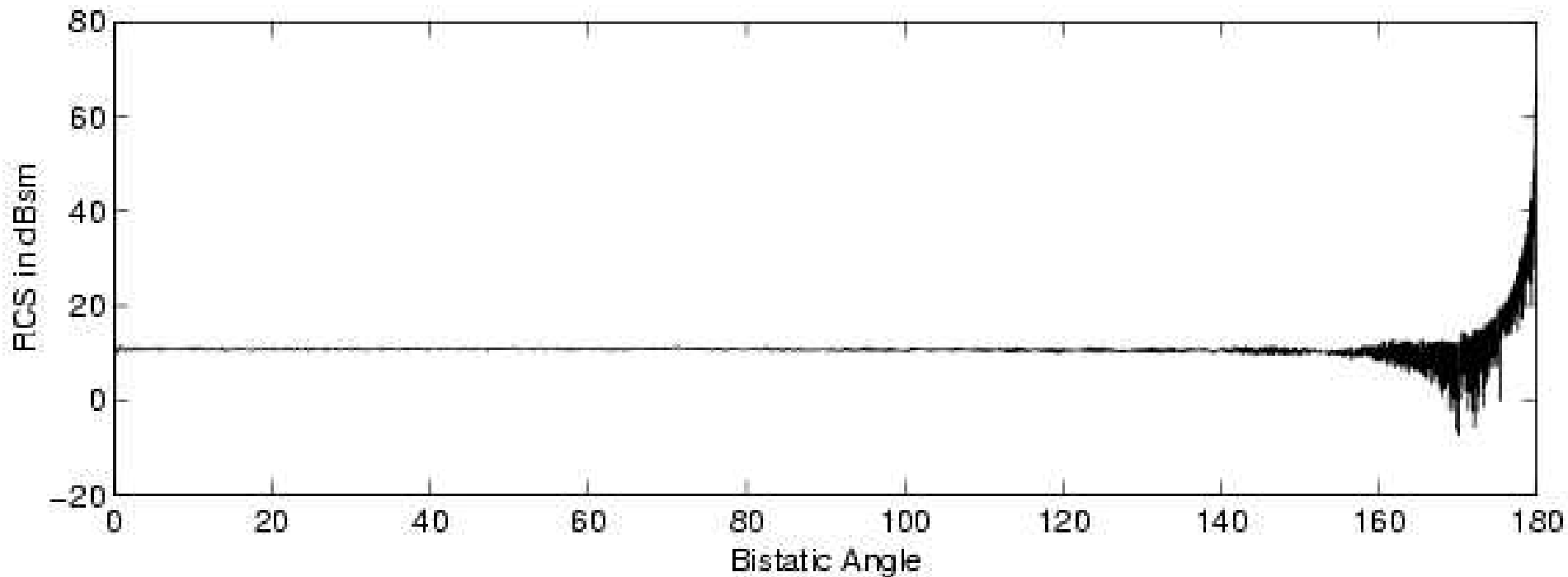
Very Large Scale Problem – VFY-218 (S. Velamparambil)

- Frequency = 8 GHz; $N = 10,186,446$
- Time for matrix-vector products: 119 s on 126 processors
- Total solution time: 7 hrs and 25 mins (2 rhs)

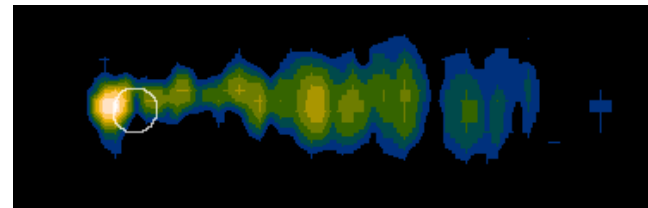
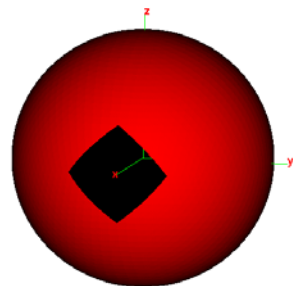
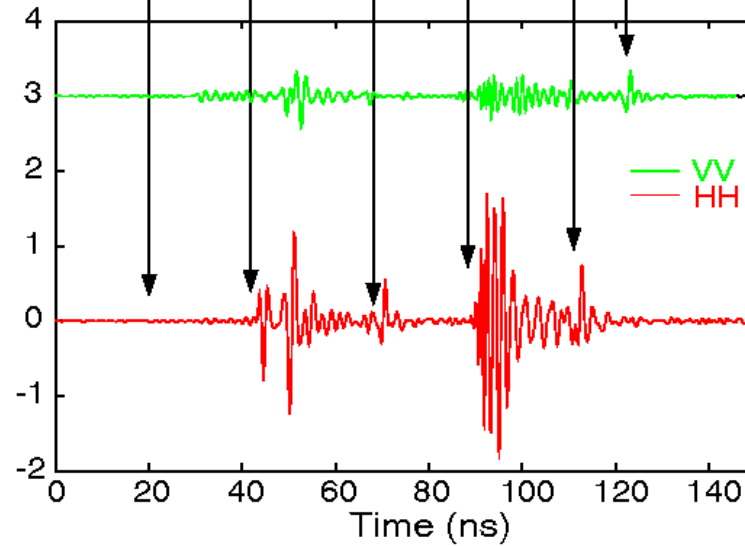
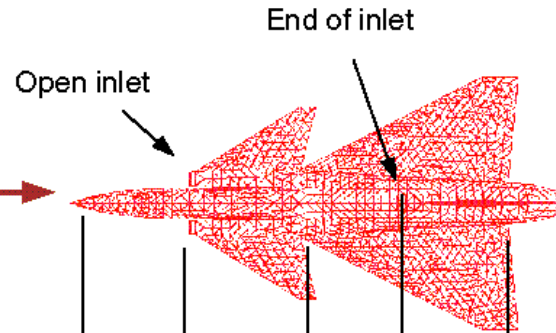
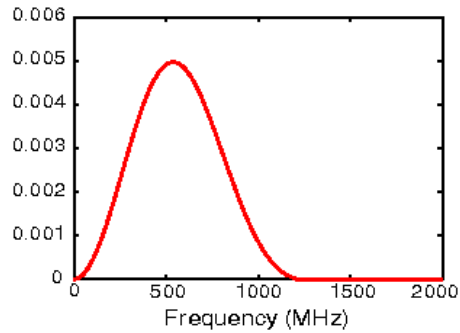
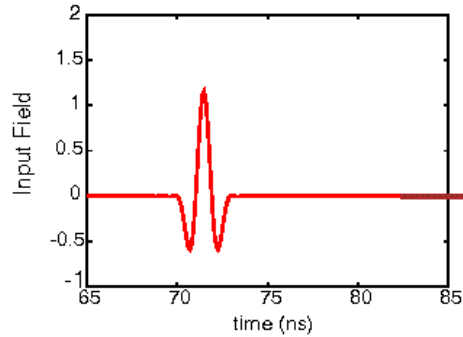
VFY-218 at 8 GHz – BISTATIC Broadside Illumination – VV and HH Polarizations



ScaleME – 20 Million Unknowns 200 λ Sphere (L. Hastriter, AFIT)



VFY218 - Nose on Time Domain



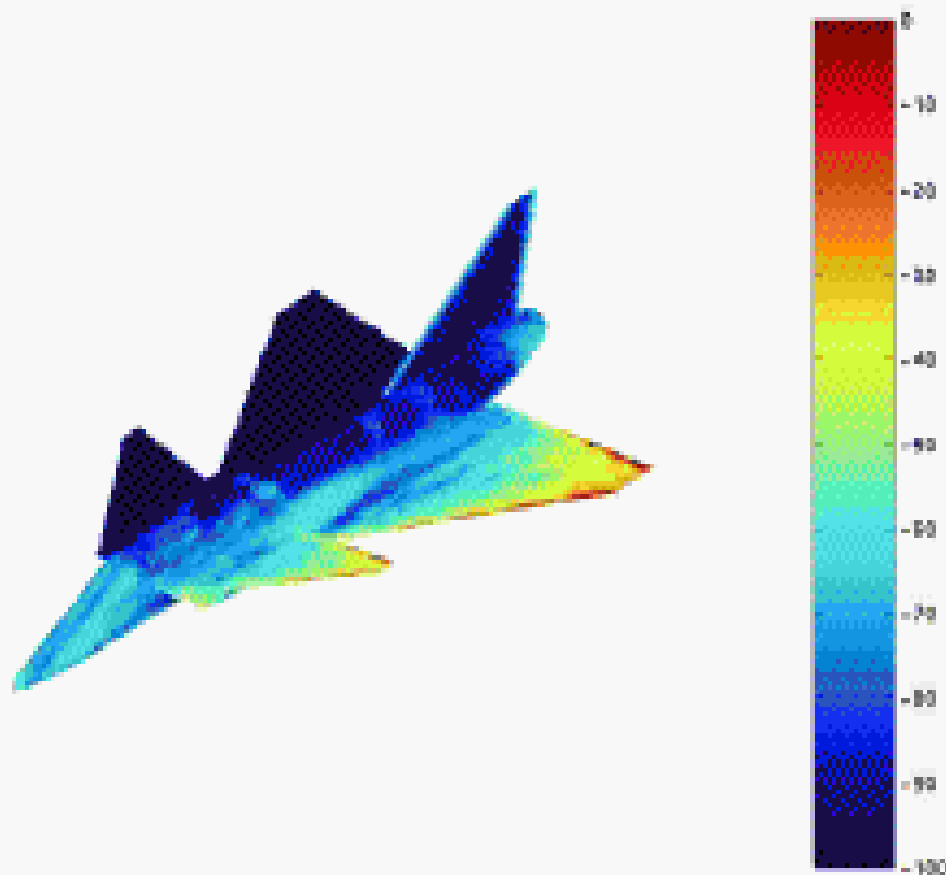
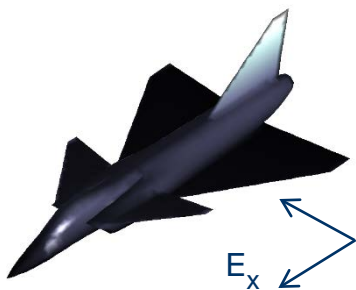
JM Song 2000

Embarrassing parallelism for multi-frequencies.

VFY 218: Current Distribution (PWTD, E. Michielssen)

Unknowns : 45492

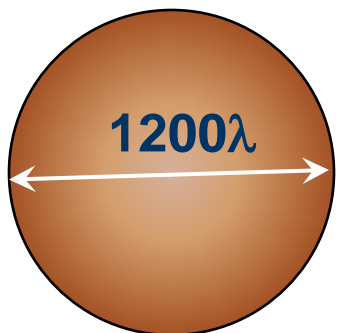
Frequency: 150 - 350 MHz



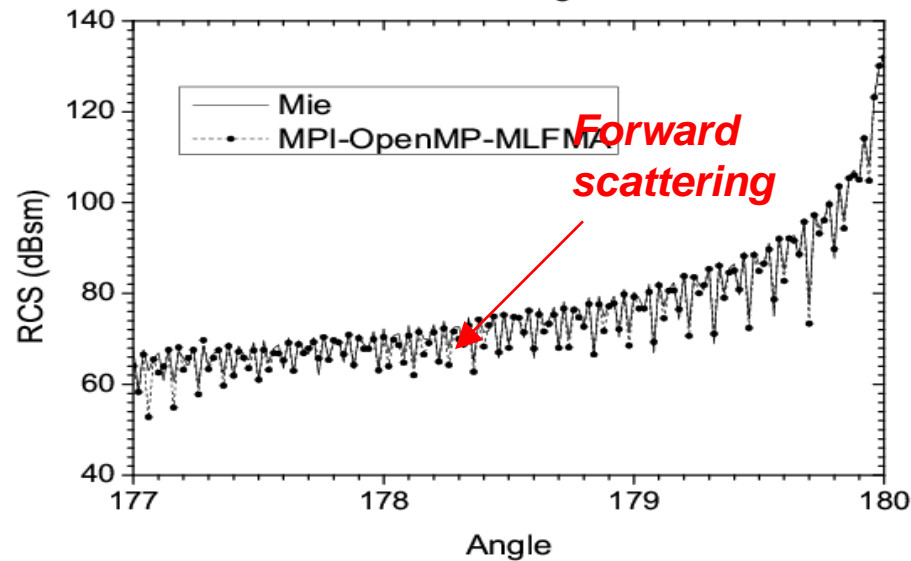
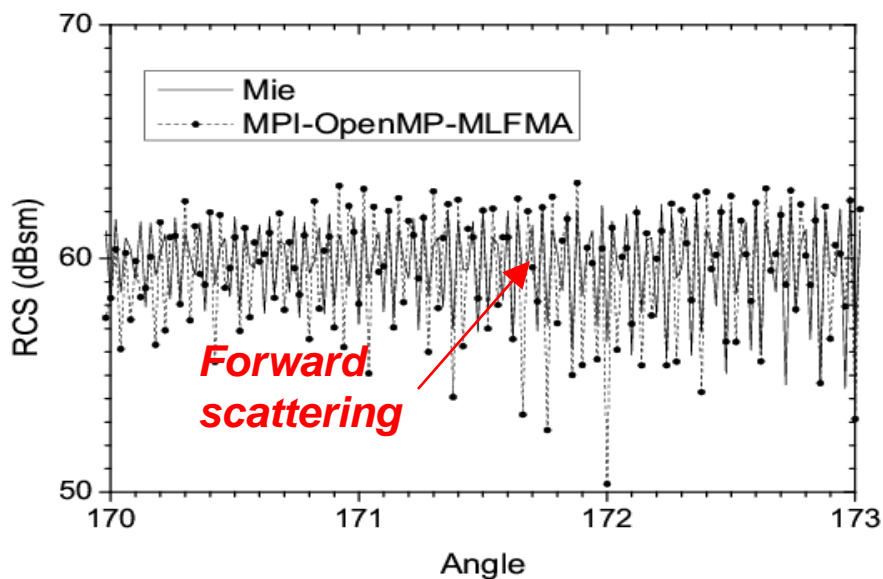
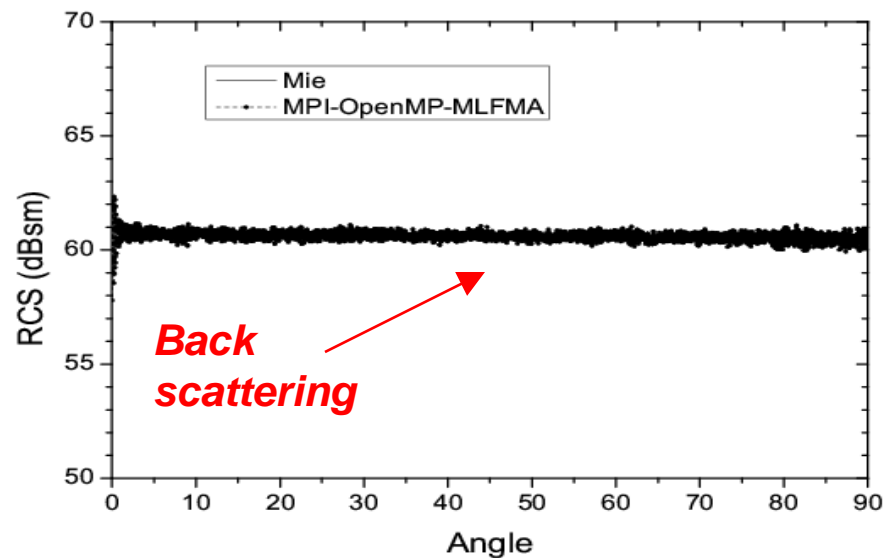
Latest Research Result (Parallel MLFMA) April 2011

X. M. Pan and X. Q. Sheng

Sphere 1,063,706,700 Unknowns

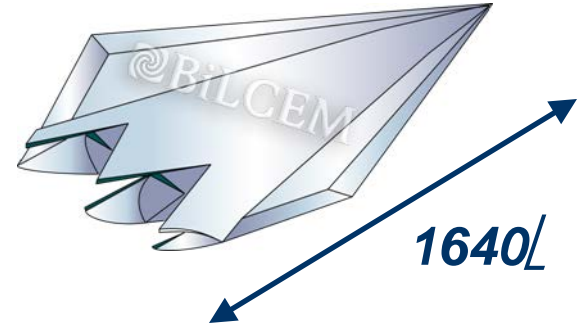


CPU * Thread	200*8
MLFMA Levels	13
Memory (TB)	3.9
Time (min)	131
RMS (dBsm)	< 0.8





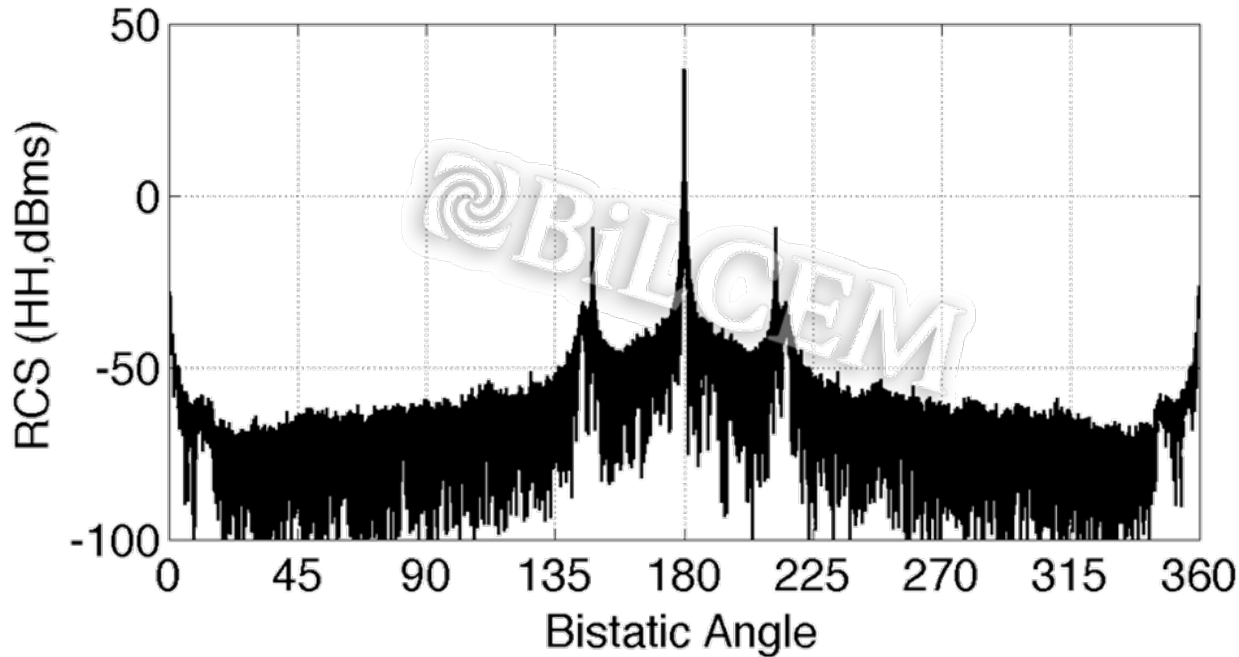
PEC Flamme
538,967,040 Unknowns



Parameters
2 digit, 10^{-3} res. Error
PW: 0H

Total Time: 42.7 hours
(16 x 4 = 64 processes)

1.87 GHz - L7555

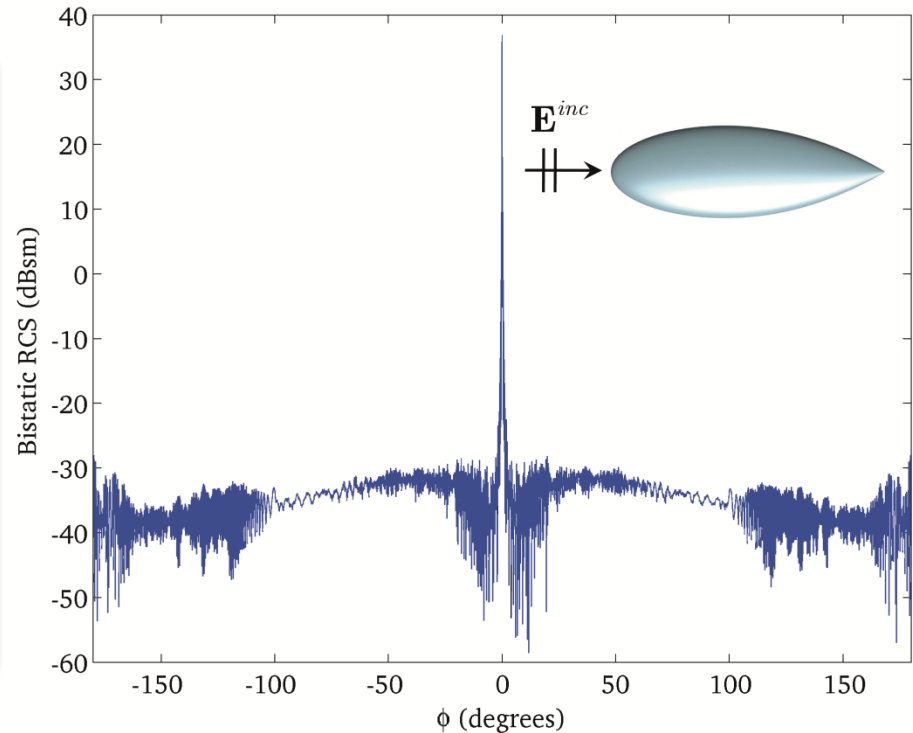


1.3 billion unknowns out of core solver, 2013

Spain

1,042,977,546 unknowns

- NASA Almond at 3 THz
- **ICTS HPC resource petition**
- 64 nodes of FinisTerae supercomputer (1024 parallel processors)
- 5 TB of total memory
- 8 iterations GMRES(80)
- 35 hours of execution
- Residue: 0.023



2. J.M. Taboada, L. Landesa, M.G. Araújo, J. Bértolo, F. Obelleiro, J.L. Rodríguez, J. Rivero, G. Gajardo-Silva, "Supercomputer solutions of extremely large problems in electromagnetics: from ten million to one billion unknowns", *European Conference on Antennas and Propagation (EUCAP 2011)*, Rome (Italy), 11-15 de abril, 2011.
3. J. M. Taboada, M. G. Araújo, F. Obelleiro, J. L. Rodríguez, L. Landesa, "MLFMA-FFT parallel algorithm for the solution of extremely large problems in electromagnetics," submitted for publication in *Proceedings of the IEEE*.

Extremely Large Problem—B. Michiels, J. Fostier, I. Bogaert, D. DeZutter (Belgium, 2013)

	Small PEC sphere	Large PEC sphere
Sphere diameter d	40.03λ	1801.25λ
Integral Equation (IE)	Combined Field IE	Combined Field IE
RWG discretization	$\lambda/10$	$\lambda/10$
Total number of unknowns N	6 027 555	3 053 598 633
Total number of CPU-cores P	1 ... 4096	4096
Total memory usage	36.31 GByte ($P = 1$)	24.9 TByte
Number of MLFMA-levels	10	15
Minimal box size	0.2λ	0.2λ
Sampling rate at highest level	5 257 848	5 121 262 968
Krylov method	TFQMR	TFQMR
Block-Jacobi preconditioner	lowest MLFMA-level	lowest MLFMA-level
MLFMA and iterative precision	10^{-2}	10^{-2}
Number of iterations	23	150
Time per iteration	59m 38s ($P = 1$)	14m 38s
Simulation error ϵ	1.03%	1.18%

Table 8.1: Simulation details

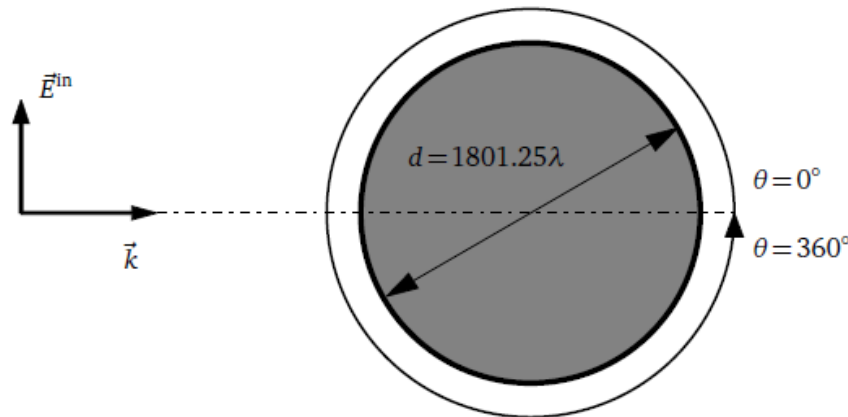
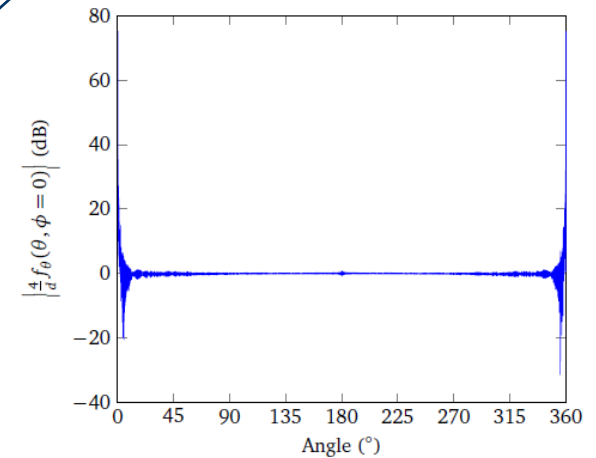
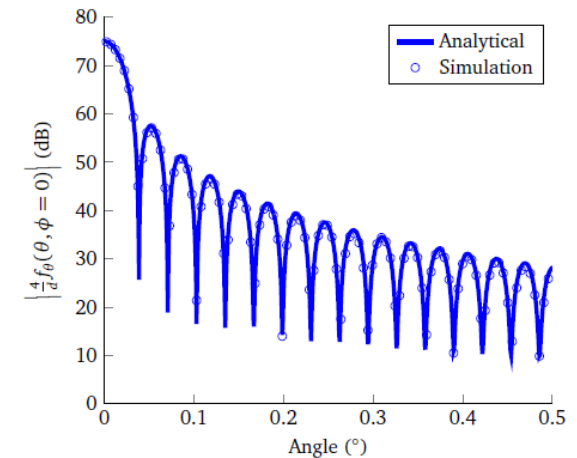


Figure 8.1: Representation of the scattering problem where a plane wave impinges on a PEC sphere with a diameter $d = 1801.25\lambda$. Using a $\lambda/10$ -discretization, this problem is converted into a MoM-MLFMA simulation that contains 3 053 598 633 unknowns.

3 billion unknowns



(a) Full θ -range ($0^\circ \dots 360^\circ$) in 71 564 sampling points.

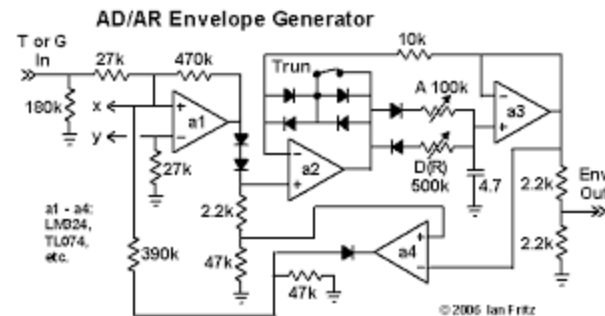


(b) Forward scattering direction ($\theta = 0^\circ \dots 0.5^\circ$).

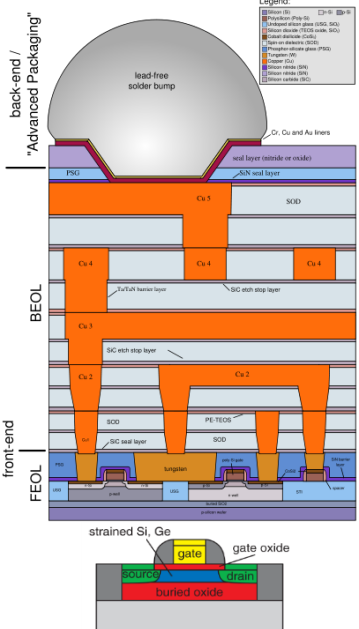
Figure 8.2: The absolute value of the normalized radiation pattern $\frac{1}{d}f_\theta(\theta, \phi = 0)$ for a PEC sphere with a diameter $d = 1801.25\lambda$.

Present CEM Needs for CPU Design

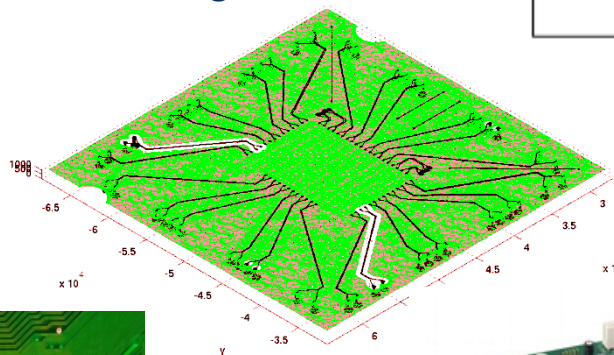
- Multi-scale and multi-physics.
- Parameter extraction replaces real-world structures with circuit models.
- Circuit equations generally solved with SPICE.
- Or solved directly with electromagnetic solvers.



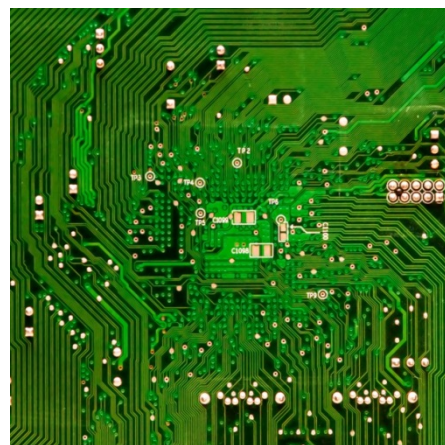
Chip



Package



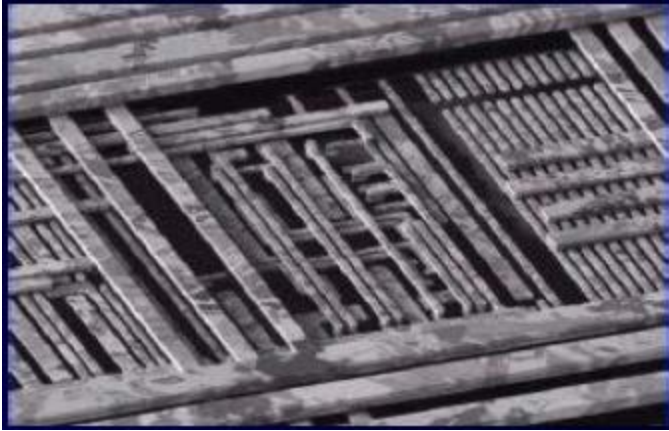
Chassis



Supported by Intel SRC and HKG
Area of Excellence

Solutions to Multi-Scale Multi-EM Physics

- Long wavelength problems for the circuits industry;



- Augmented Electric Field Integral Equation (A-EFIE);
- Equivalence Principle Algorithm (EPA) for Domain Decomposition Method (DDM);

Mixed Form Fast Multipole Algorithm--MF-FMA (Non-Diagonal to Diagonal Translation) w/ L.J. Jiang

$$\begin{aligned} [\alpha_{LL'}(\mathbf{r}_{ji})]_{L \times L'} &= [\beta_{LL_1}(\mathbf{r}_{jJ_1})]_{L \times L_1} \\ &\cdot [\beta_{L_1L_2}(\mathbf{r}_{J_1J_2})]_{L_1 \times L_2} \cdot [\beta_{L_2L_3}(\mathbf{r}_{J_2J_3})]_{L_2 \times L_3} \\ &\cdot [D]_{S_4 \times L_3}^\dagger \end{aligned}$$

Low frequency
Circuit Physics

Transformer

$$\begin{aligned} &\cdot \text{diag} [e^{ik \cdot \mathbf{r}_{J_3J_4}}]_{S_4 \times S_4} \cdot [I]_{S_5 \times S_4}^T \\ &\cdot \text{diag} [e^{ik \cdot \mathbf{r}_{J_4J_5}}]_{S_5 \times S_5} \\ &\cdot \text{diag} [\tilde{T}(\Omega_{S_5}, \mathbf{r}_{J_5I_5}) w_{S_5}]_{S_5 \times S_5} \\ &\cdot \text{diag} [e^{ik \cdot \mathbf{r}_{I_5I_4}}]_{S_5 \times S_5} \cdot [I]_{S_5 \times S_4} \\ &\cdot \text{diag} [e^{ik \cdot \mathbf{r}_{I_4I_3}}]_{S_4 \times S_4} \end{aligned}$$

Mid frequency

Wave Physics

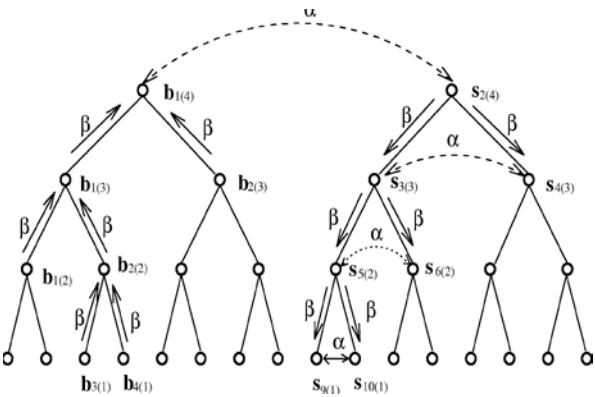
$$\cdot [D]_{S_4 \times L_3}$$

Transformer

$$\begin{aligned} &\cdot [\beta_{L_3L_2}(\mathbf{r}_{I_3I_2})]_{L_3 \times L_2} \cdot [\beta_{L_2L_1}(\mathbf{r}_{I_2I_1})]_{L_2 \times L_1} \\ &\cdot [\beta_{L_1L'}(\mathbf{r}_{I_1i})]_{L_1 \times L'} \end{aligned}$$

Low frequency

Circuit Physics



A-EFIE Formulation, and LF and Broadband Scheme

- Electric field integral equation (EFIE)
 - Most popular w/ LF breakdown

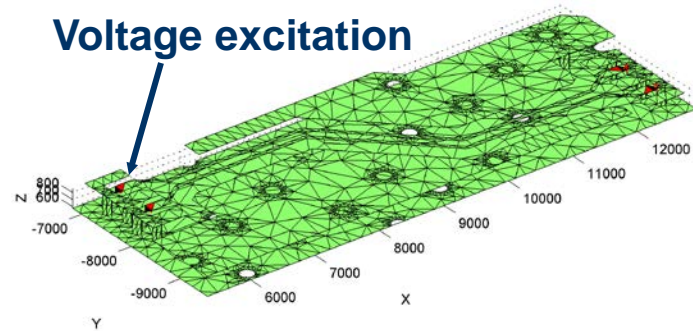
$$\bar{\mathbf{G}}(\mathbf{r}, \mathbf{r}', \omega) = \left(\bar{\mathbf{I}} + \frac{\nabla \nabla}{k^2} \right) \frac{e^{ikR}}{4\pi R} \quad \left(ik_0 \eta_0 \bar{\mathbf{V}} + \frac{\eta_0}{ik_0} \bar{\mathbf{S}} \right) \cdot \mathbf{J} = \mathbf{b}$$

$$\bar{\mathbf{S}} = \bar{\mathbf{D}}^T \cdot \bar{\mathbf{P}} \cdot \bar{\mathbf{D}}$$

$\bar{\mathbf{P}}$ Patch-based scalar potential matrix

$\bar{\mathbf{D}}$ Incidence matrix of graph G

$$\bar{\mathbf{D}} \cdot \mathbf{J} = ik_0 c_0 \boldsymbol{\rho}$$

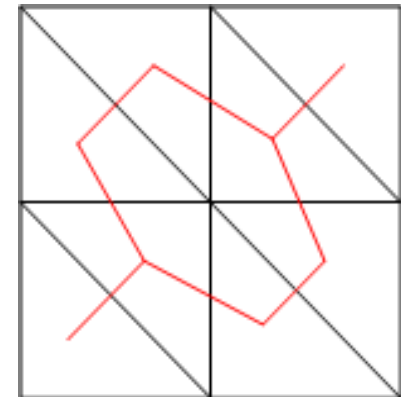


- Augmented EFIE [1] KVL and KCL

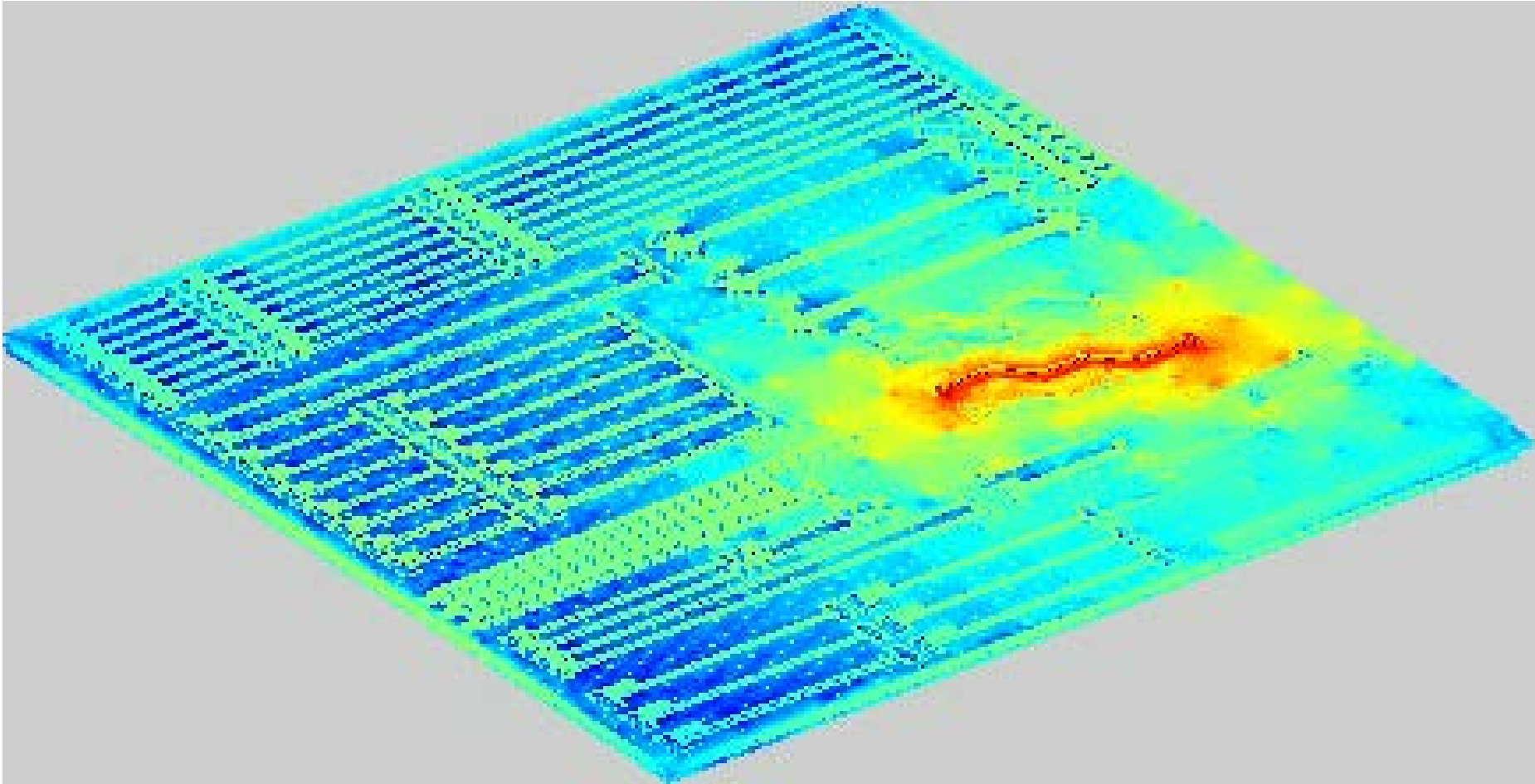
$$\begin{array}{l} \text{KVL} \\ \text{KCL} \end{array} \begin{bmatrix} \bar{\mathbf{V}} & \bar{\mathbf{D}}^T \cdot \bar{\mathbf{P}} \\ \bar{\mathbf{D}} & k_0^2 \bar{\mathbf{U}} \end{bmatrix} \cdot \begin{bmatrix} ik_0 \mathbf{J} \\ c_0 \boldsymbol{\rho} \end{bmatrix} = \begin{bmatrix} \eta_0^{-1} \mathbf{b} \\ \mathbf{0} \end{bmatrix}$$

- Charge neutrality: $\sum_n \rho_n = 0$

graph G



Movie of Current—3 GHz



Multi-scale Package Solved with A-EFIE on a Single CPU

Recent Advances—A-EFIE for Lossy Dielectrics with Tian XIA and Intel Support

- Both the external and internal EFIE are augmented by the current continuity equation

$$\begin{bmatrix} \bar{\mathbf{V}}_{ext} & \bar{\mathbf{K}}_{ext} & \bar{\mathbf{D}}^T \cdot \bar{\mathbf{P}}_{ext} \cdot \bar{\mathbf{B}} \\ \bar{\mathbf{V}}_{int} & \bar{\mathbf{K}}_{int} & \bar{\mathbf{D}}^T \cdot \bar{\mathbf{P}}_{int} \cdot \bar{\mathbf{B}} \\ \bar{\mathbf{F}} \cdot \bar{\mathbf{D}} & 0 & k_0^2 \bar{\mathbf{I}} \end{bmatrix} \cdot \begin{bmatrix} ik_0 \mathbf{J} \\ \eta_0^{-1} \mathbf{M} \\ c_0 \boldsymbol{\rho}_r \end{bmatrix} = \begin{bmatrix} -\eta_0^{-1} \mathbf{b} \\ 0 \\ 0 \end{bmatrix}$$

Lossy Conductor Simulations

- Use a novel integration scheme to calculate the interaction matrix element for the internal lossy media^[1].
- This scheme converts the surface integrals on a triangle into line integrals along the 3 edges of the triangle.

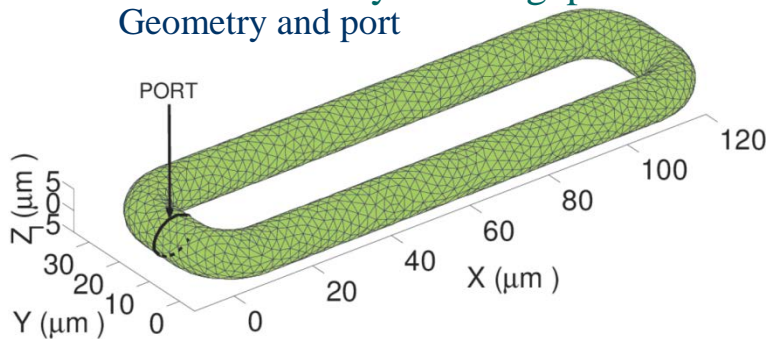
[1] Z. G. Qian, W. C. Chew, and R. Suaya, "Generalized impedance boundary condition for conductor modeling in surface integral equation," *IEEE Trans. Antennas Propag.*, vol. 55, no. 11, pp. 2354–2364, 2007.

Conductors as Lossy Dielectrics (High Conductivity Case)

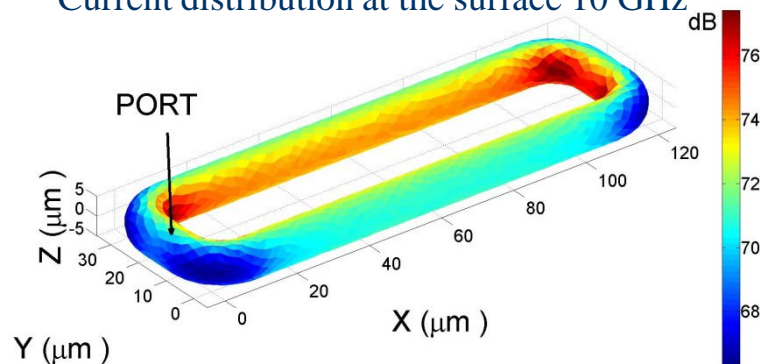
- Numerical simulation:

- A conductive transmission:

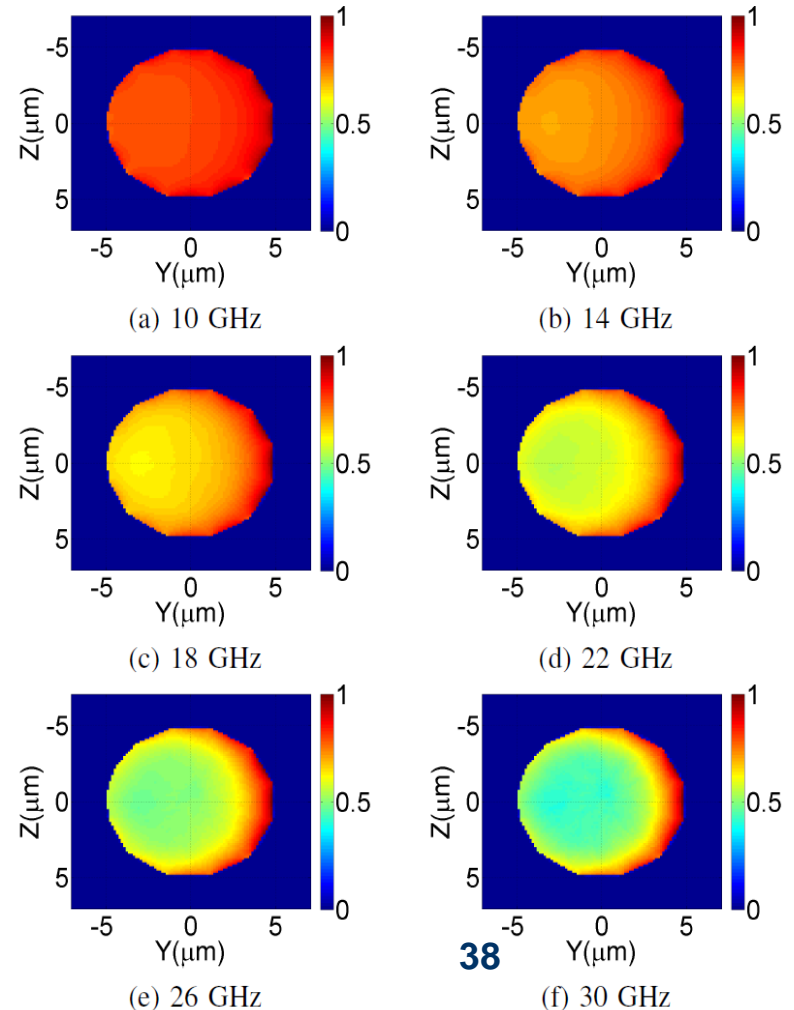
- Conductivity $\sigma = 10^6$ S/m (close to Nichrome's conductivity)
 - Excited by a delta gap source at the port



Current distribution at the surface 10 GHz



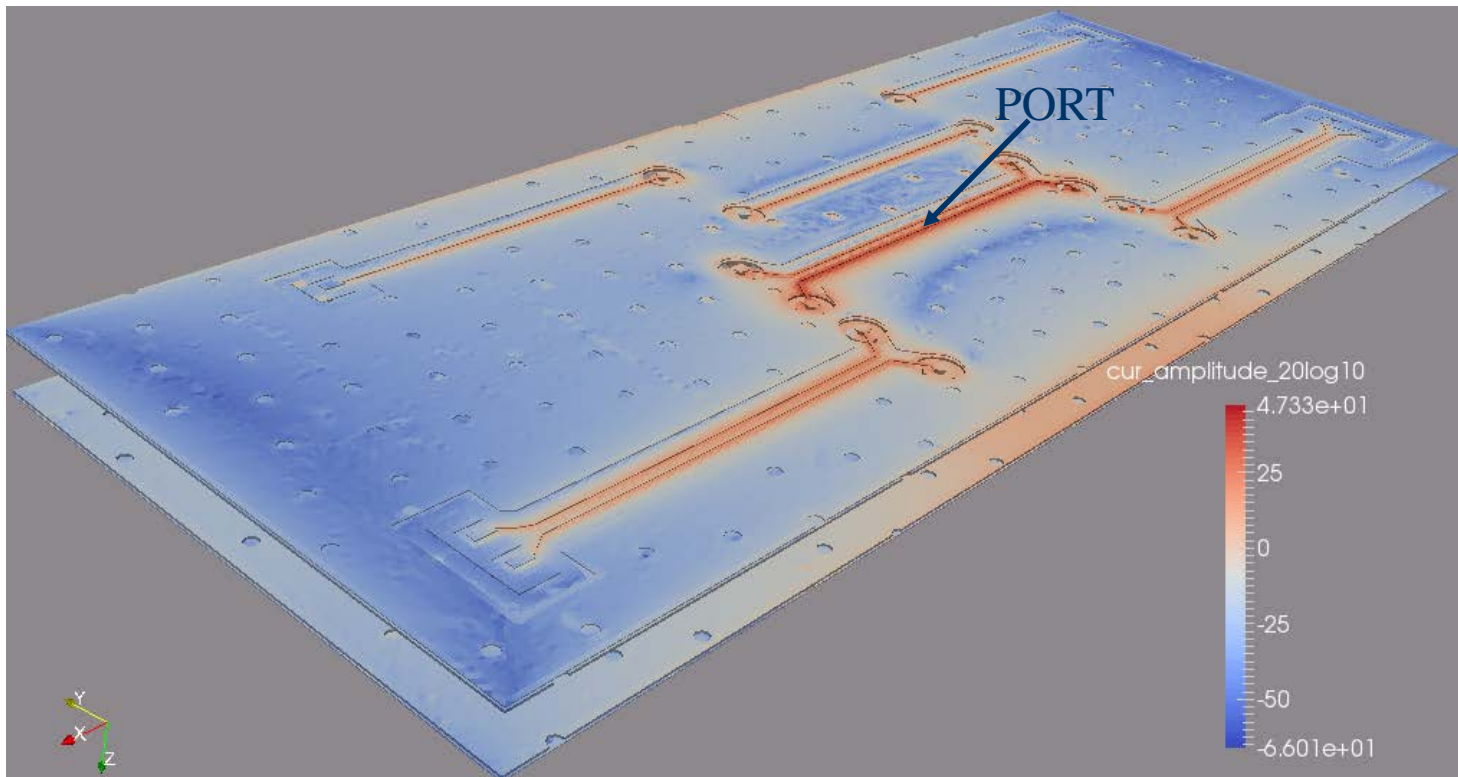
Current at the cross section
(center of the transmission line)



Simulation Results of Real World Problems

- Simulation results:
 - This problem is solved at 2 GHz. The current distribution is shown.

Current distribution at 2GHz



Modal Expansion Methods (Qi Dai)

- Natural mode expansions;
- Characteristics mode expansions;
- Eigenmode expansions;
- Modal order reduction:
 - **Circuit analysis;**
 - **Antenna analysis;**
 - **Target ID: K pulse, E pulse etc.;**
 - **Circuit/waveguide/cavity QED (quantum electrodynamics).**
 - Not “quod erat demonstrandum”, nor “quite easily done.”

Integral Equation Based Formulation

(Q. Dai)

Electric field IE (EFIE) impedance matrix for PEC scatterers

$$\begin{aligned} Z_{mn} &= i\omega\mu \langle \mathbf{f}_m, \overline{\mathbf{G}}, \mathbf{f}_n \rangle \\ &= i\omega\mu \int_s d\mathbf{r} \mathbf{f}_m(\mathbf{r}) \cdot \int_s \overline{\mathbf{G}}(\mathbf{r}, \mathbf{r}') \cdot \mathbf{f}_n(\mathbf{r}') d\mathbf{r}' \end{aligned}$$

- Natural modes

$$\overline{\mathbf{Z}} \cdot \mathbf{J} = 0$$

$$[\overline{\mathbf{Z}}(\omega_n)] = 0$$

- Complex ω_n to solve
- Nonlinear equation
- Singularity expansion method (Carl Baum)

- Characteristic modes theory (CMT)

$$\overline{\mathbf{X}} \mathbf{J}_n = \lambda_n \overline{\mathbf{R}} \mathbf{J}_n$$

$$\overline{\mathbf{Z}} = \overline{\mathbf{R}} + i\overline{\mathbf{X}}$$

- Fixed real ω_n
- Generalized eigenvalue problem
- Converted to standard eigenvalue problem when solved with iterative eigensolvers (ARPACK)

Integral Equation Based Formulation

$$\bar{\mathbf{Z}}_C \mathbf{I} = \mathbf{F}_{inc}$$

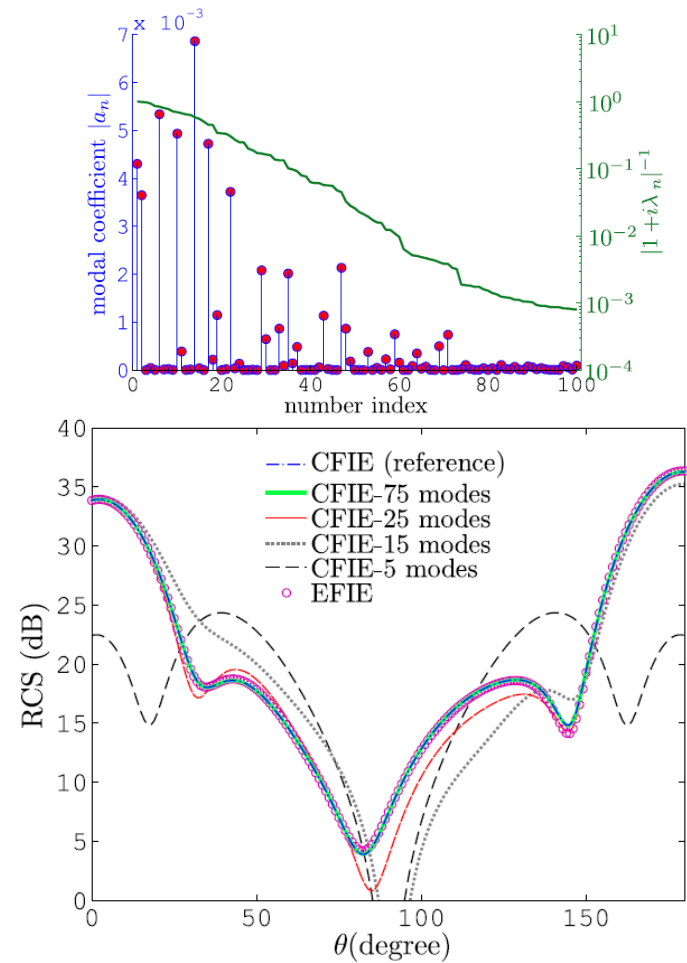
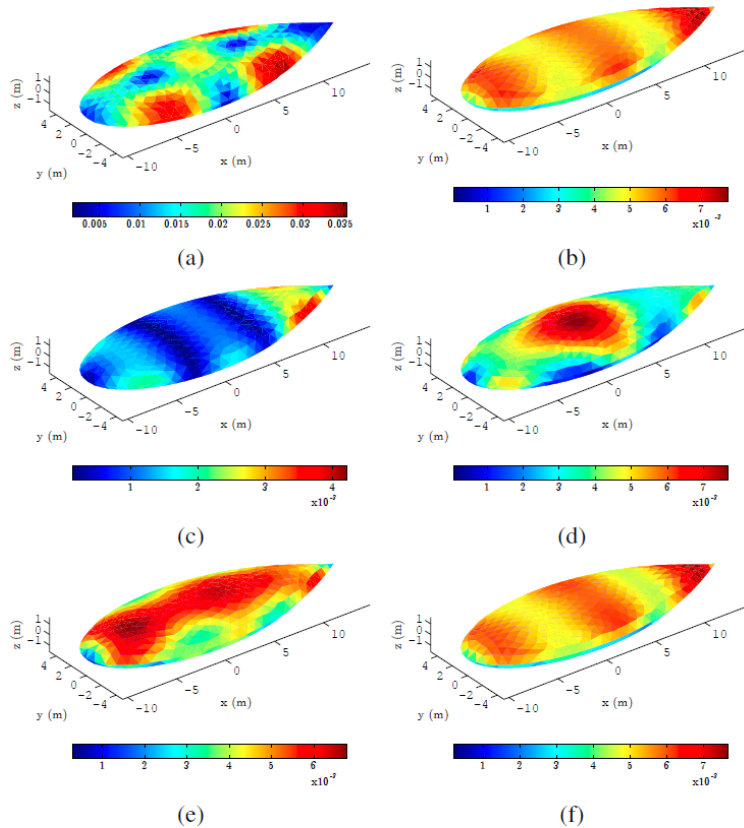
$$[\alpha \mathcal{Z}_E(\mathbf{r}, \mathbf{r}') + (1 - \alpha)\eta \mathcal{Z}_H(\mathbf{r}, \mathbf{r}')] \cdot \mathbf{J}(\mathbf{r}')$$

$$\bar{\mathbf{Z}}_C = \alpha \bar{\mathbf{Z}}_E + (1 - \alpha)\eta \bar{\mathbf{Z}}_H$$

$$= -\alpha \hat{\mathbf{n}} \times \mathbf{E}_{inc}(\mathbf{r}) + (1 - \alpha)\eta \bar{\mathbf{I}}_t \cdot \mathbf{H}_{inc}(\mathbf{r})$$

- Modal expansion $\bar{\mathbf{Z}}_C \mathbf{J}_n = (1 + i\lambda_n) \bar{\mathbf{K}}_C \mathbf{J}_n$ $\bar{\mathbf{Z}}_C^T \mathbf{J}_n^a = (1 + i\lambda_n) \bar{\mathbf{K}}_C^T \mathbf{J}_n^a$

$$\mathbf{I} = \bar{\mathbf{J}} \mathbf{a} \quad \mathbf{a} = (\bar{\mathbf{\Sigma}})^{-1} (\bar{\mathbf{J}}^a)^T \mathbf{F}_{inc}$$



Integral Equation Based Formulation

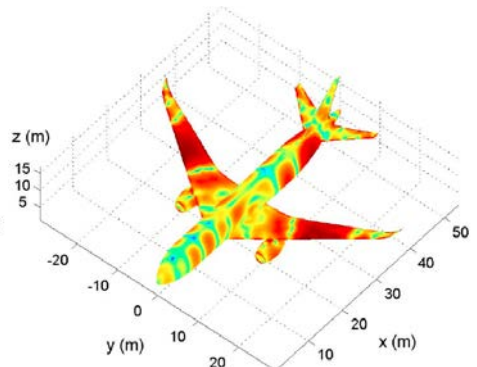
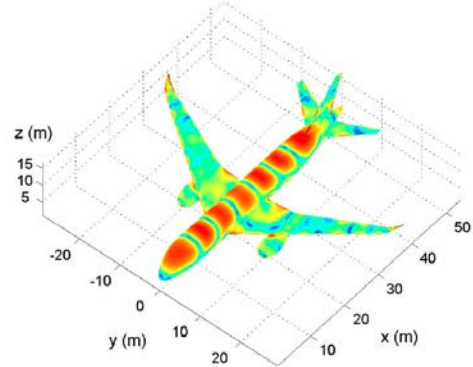
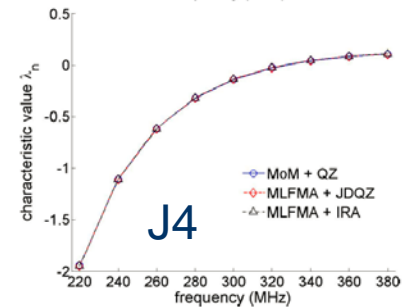
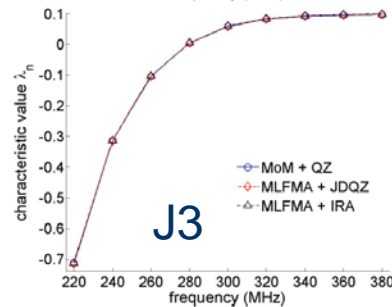
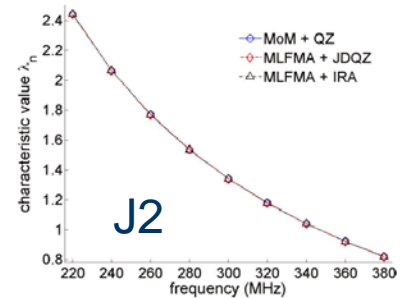
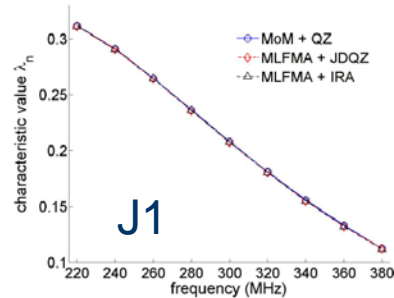
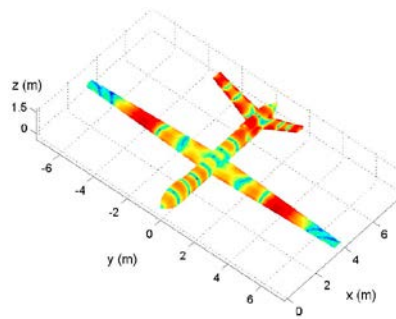
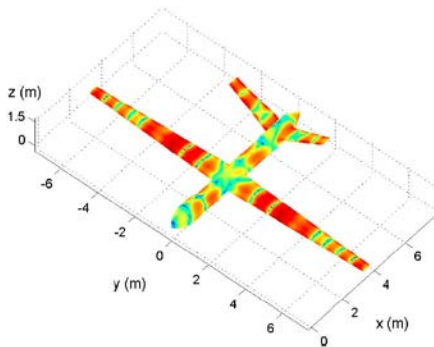
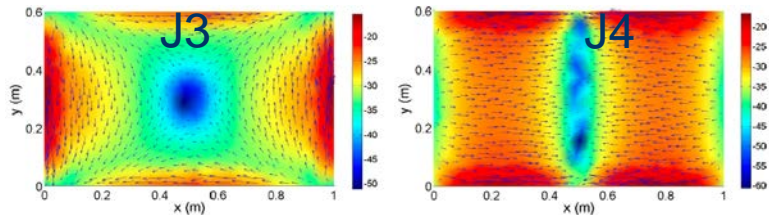
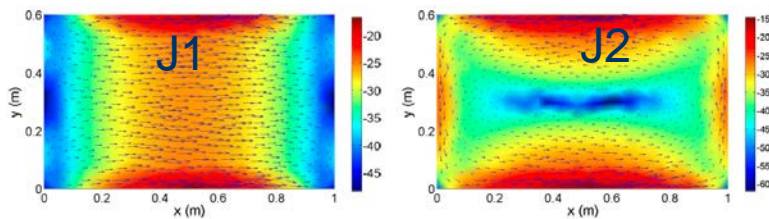
- Fast Multipole Algorithm

$$\frac{\cos(kr_{ij})}{r_{ij}} = \frac{ik}{4\pi} \int d^2\hat{k} e^{ik \cdot (\mathbf{r}_{im} + \mathbf{r}_{m'j})} \alpha_{mm'}^{\mathfrak{S}}(\mathbf{k}, \mathbf{r}_{mm'})$$

$$\alpha_{mm'}^{\mathfrak{S}}(\mathbf{k}, \mathbf{r}_{mm'}) = i \sum_{l=0}^L i^l (2l+1) y_l(kr_{mm'}) P_l(\hat{\mathbf{k}} \cdot \hat{\mathbf{r}}_{mm'})$$

$$\frac{\sin(kr_{ij})}{r_{ij}} = \frac{ik}{4\pi} \int d^2\hat{k} e^{ik \cdot (\mathbf{r}_{im} + \mathbf{r}_{m'j})} \alpha_{mm'}^{\mathfrak{R}}(\mathbf{k}, \mathbf{r}_{mm'})$$

$$\alpha_{mm'}^{\mathfrak{R}}(\mathbf{k}, \mathbf{r}_{mm'}) = -i \sum_{l=0}^L i^l (2l+1) j_l(kr_{mm'}) P_l(\hat{\mathbf{k}} \cdot \hat{\mathbf{r}}_{mm'})$$



A-Φ Formulation: Null space elimination by a generalized gauge operator (Y.L. Li, S. Sun)

➤ Finite element discretization

- Differential form interpretation of the gauge operator

E and **A**: 1-form variables

$$\mathbf{f}(\mathbf{r}) = \sum_{n=1}^{N_e} x_n \boldsymbol{\omega}_n(\mathbf{r})$$

mapping between differential forms:

$$\begin{array}{ccccccc} \mathbf{A} & \xrightarrow{\star_\epsilon} & \epsilon \mathbf{A} & \xrightarrow{\nabla \cdot} & \nabla \cdot \epsilon \mathbf{A} & \xrightarrow{\star_\mu, \star_\epsilon} & \frac{1}{\mu \epsilon^2} \nabla \cdot \epsilon \mathbf{A} \\ \downarrow & & \downarrow & & \downarrow & & \downarrow \\ \text{1-form} & & \text{2-form} & & \text{3-form} & & \text{0-form} \end{array}$$

$$\frac{1}{\mu \epsilon^2} \nabla \cdot \epsilon \mathbf{f}(\mathbf{r}) = \sum_{n=1}^{N_n} d_n \lambda_n(\mathbf{r})$$

$$\mathcal{L} \mathbf{f} = \nabla \times \frac{1}{\mu} \nabla \times \mathbf{f} - \epsilon \nabla \frac{1}{\alpha \mu \epsilon^2} \nabla \cdot \epsilon \mathbf{f}$$

gauge operator

$$\bar{\mathbf{K}} \mathbf{x} = \left(\bar{\mathbf{K}}_1 \left[-\bar{\mathbf{K}}_3 \bar{\mathbf{G}}_{NN}^{-1} \bar{\mathbf{G}}_{NE} \right] \right) \mathbf{x}$$

double-curl operator

$$\bar{\mathbf{K}}'_3 = -\bar{\mathbf{K}}_3 \bar{\mathbf{G}}_{NN}^{-1} \bar{\mathbf{G}}_{NE}$$

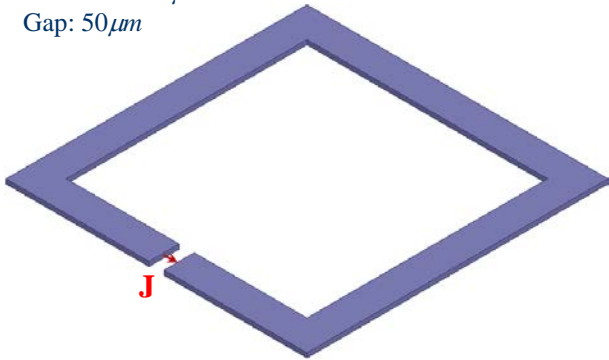
sparse approximate inverse (SAI)

nearly-diagonal matrix

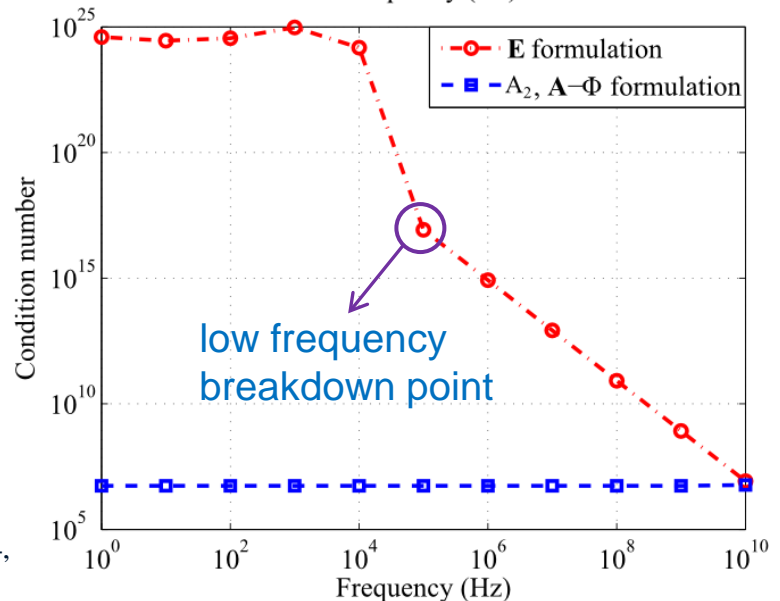
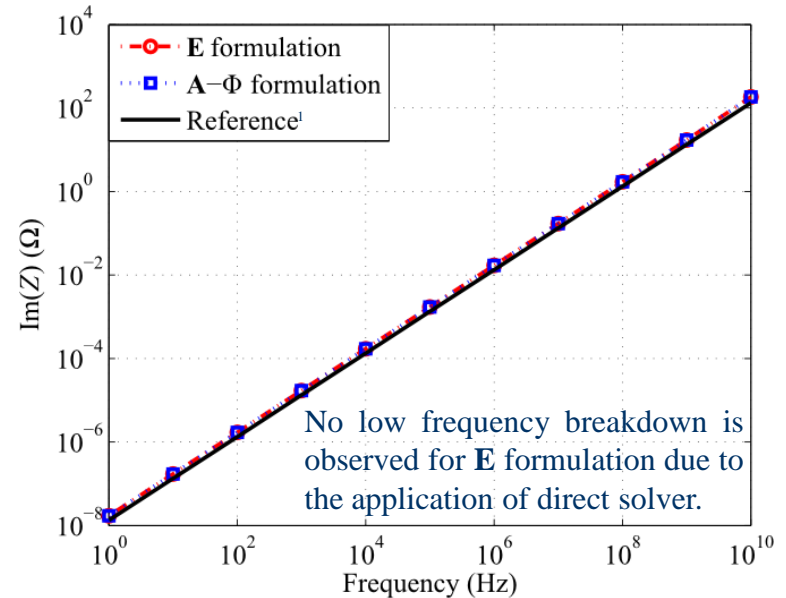
$\mathbf{A}\text{-}\Phi$ formulation for low frequency circuits (FEM)

- Square loop structure (PEC)

Loop size: $1000\mu\text{m}$ (outer), $800\mu\text{m}$ (inner)
 Thickness: $15\mu\text{m}$
 Gap: $50\mu\text{m}$



frequency (Hz)	electric size of the minimum mesh
1×10^{10}	5.0000×10^{-4}
1×10^7	5.0000×10^{-7}
1×10^4	5.0000×10^{-10}
1×10^0	5.0000×10^{-14}



¹S. S. Mohan, M. M. Hershenson, S. P. Boyd, and T. H. Lee, "Simple accurate expressions for spiral inductances," *IEEE Journal of Solid-state Circuits*, vol. 34, pp.1419-1424, 1999.

A- Φ Formulation for Integral Equation (MOM Discretization) - **PEC (Q. Liu and S. Sun)**

Surface Charge $\hat{n} \cdot \epsilon_1 \mathbf{E}_1 = \hat{n} \cdot \epsilon_1 (i\omega \mathbf{A}_1 - \nabla \Phi_1)$
 $\hat{n} \cdot \mathbf{A}$: contribution to the surface charge.

- **-Formulation**

$$0 = \mathbf{A}_{\text{inc}}(\mathbf{r}) + \int_S dS' \left\{ \mu_1 g_1(\mathbf{r}, \mathbf{r}') \underbrace{\mathbf{J}_1(\mathbf{r}')}_{\text{RWG}} - \underbrace{\Sigma_1(\mathbf{r}')}_{\text{Pulse}} \nabla' g_1(\mathbf{r}, \mathbf{r}') \right\} \quad \mathbf{r} \in S^+$$

Testing with RWG basis

- **Φ -Formulation**

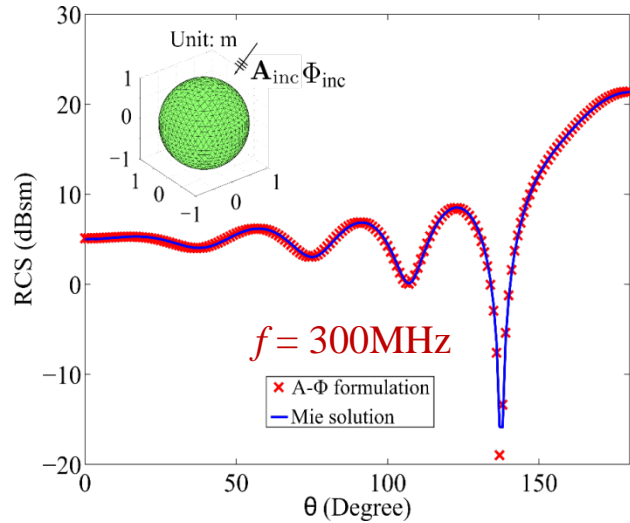
$$0 = i\omega \mu \epsilon \Phi_{\text{inc}}(\mathbf{r}) + \int_S dS' \left\{ \mu_1 g_1(\mathbf{r}, \mathbf{r}') \nabla' \cdot \underbrace{\mathbf{J}_1(\mathbf{r}')}_{\text{RWG}} + k^2 g_1(\mathbf{r}, \mathbf{r}') \underbrace{\Sigma_1(\mathbf{r}')}_{\text{Pulse}} \right\} \quad \mathbf{r} \in S^+$$

Testing with pulse basis

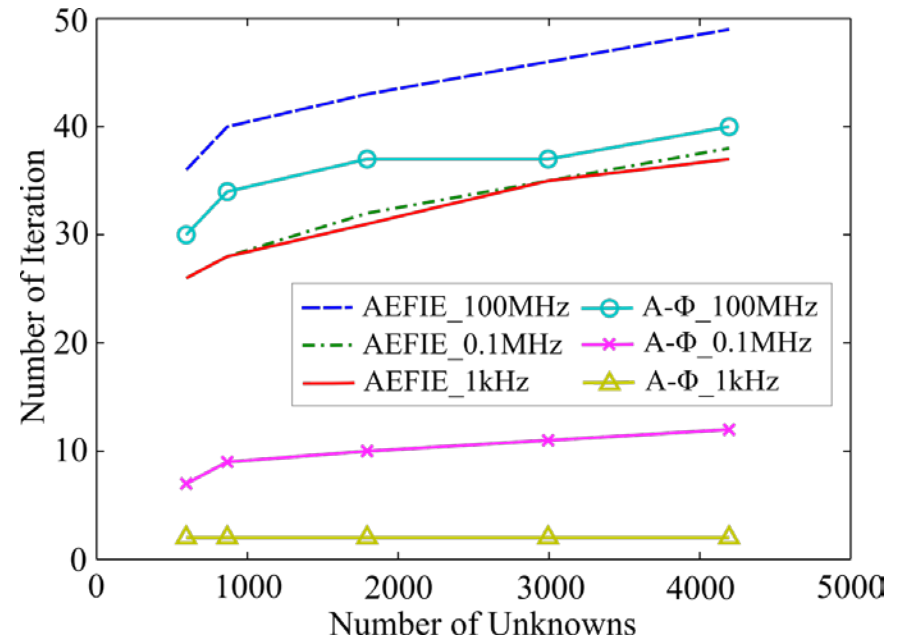
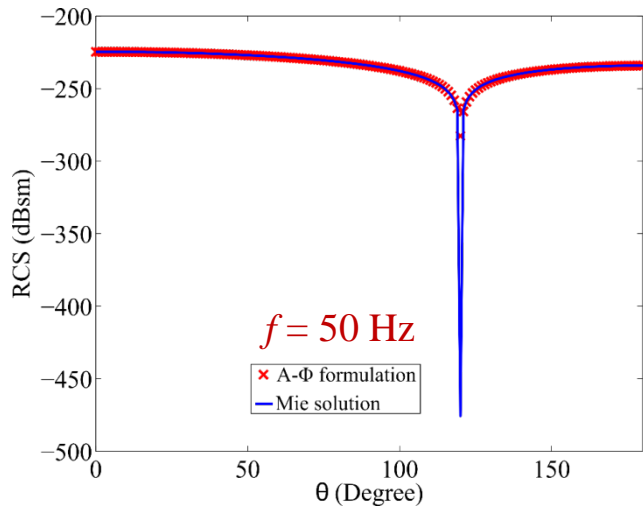
Divergence

A- Φ Formulation for Integral Equation

—Scattering Problem (Q. Liu and S. Sun)



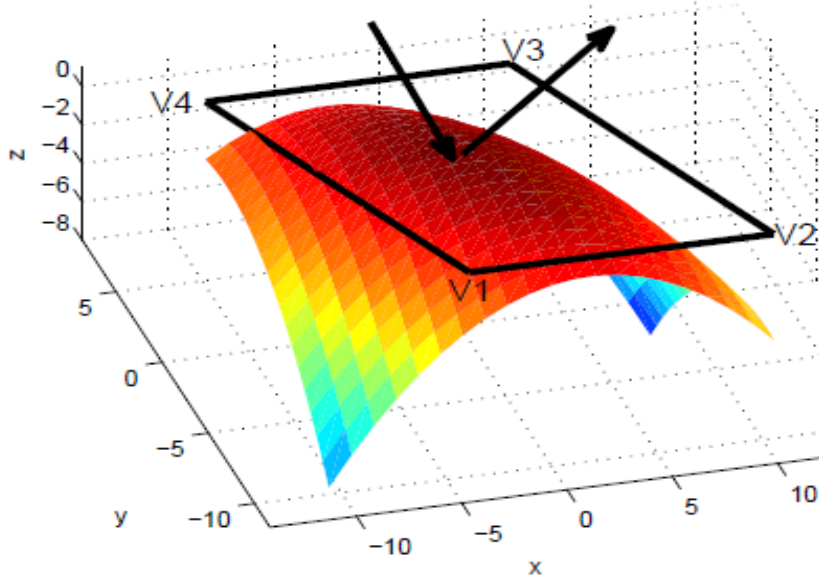
No. edges: 1568; No. patches: 2352



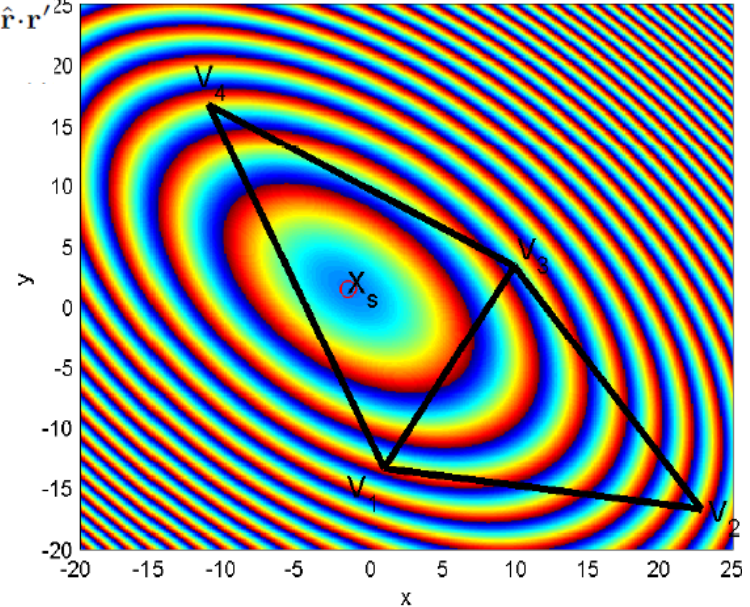
- ✓ Good accuracy at both middle and low frequencies
- ✓ Stable convergence as the mesh density increases
- ✓ Convergent faster than original A-EFIE at low frequencies

THE PO SCATTERED ELECTRIC FIELD BY THE NUMERICAL STEEPEST DESCENT METHOD –WITH Y.M. WU (FUDAN)

$$\mathbf{E}_s(\mathbf{r}) \approx \frac{ikZ_0 e^{ikr}}{4\pi r} \hat{\mathbf{r}} \times \hat{\mathbf{r}} \times \int_{\partial\Omega} dS(\mathbf{r}') [\hat{\mathbf{n}}(\mathbf{r}') \times \mathbf{H}(\mathbf{r}')] e^{-ik\hat{\mathbf{r}} \cdot \mathbf{r}'}$$



A parabolic PEC patch



The x-y quadrilateral domain

PO approximation

$$\mathbf{J}(\mathbf{r}') = \begin{cases} 2\hat{\mathbf{n}}(\mathbf{r}') \times \mathbf{H}^{(i)}(\mathbf{r}'), & \mathbf{r}' \in \partial\Omega_1 \\ 0, & \mathbf{r}' \in \partial\Omega_2 \end{cases}$$

Local tangential plane approximation

Backward scattering case

$$\mathbf{E}_s(\mathbf{r}) \approx \mathbf{E}_0^{(i)} I$$

$$I = \int_{\partial\Omega} s(\mathbf{r}') e^{ikv(\mathbf{r}')} dS(\mathbf{r}')$$

$$s(\mathbf{r}') = -\frac{ike^{ikr}}{2\pi r} \hat{\mathbf{r}}^{(i)} \cdot \hat{\mathbf{n}}(\mathbf{r}')$$

$$v(\mathbf{r}') = 2\hat{\mathbf{r}}^{(i)} \cdot \mathbf{r}'$$

High Frequency with Numerical Steepest Descent Path (NSDP) Method —Y.M. WU

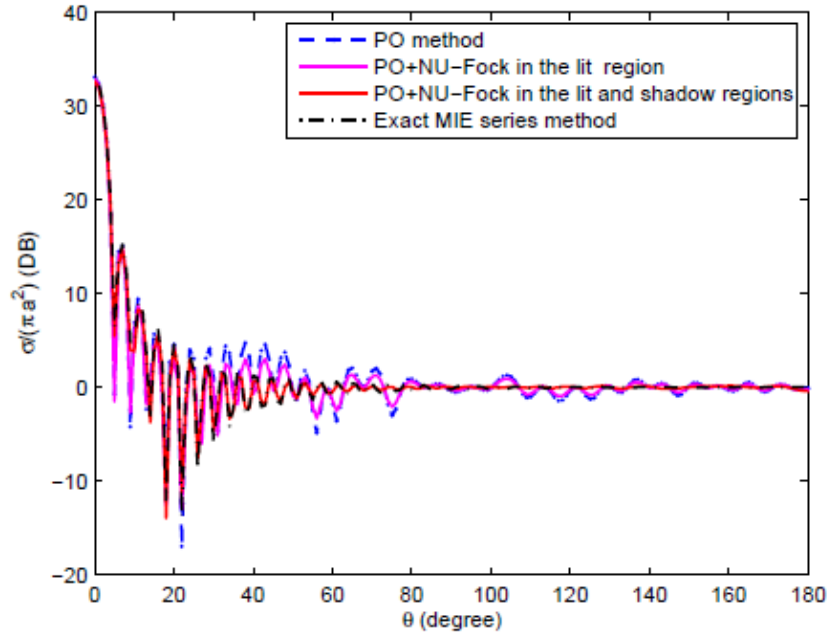


Fig. 9. The far scattered fields from the 3-D conducting sphere are produced by the PO approximation current, the summation of the PO current and the NU-Fock currents in the scatterer's lit and shadow regions, and the Mie series method, respectively. The product of the wave frequency and the radius of the sphere has the value $kR = 45$.

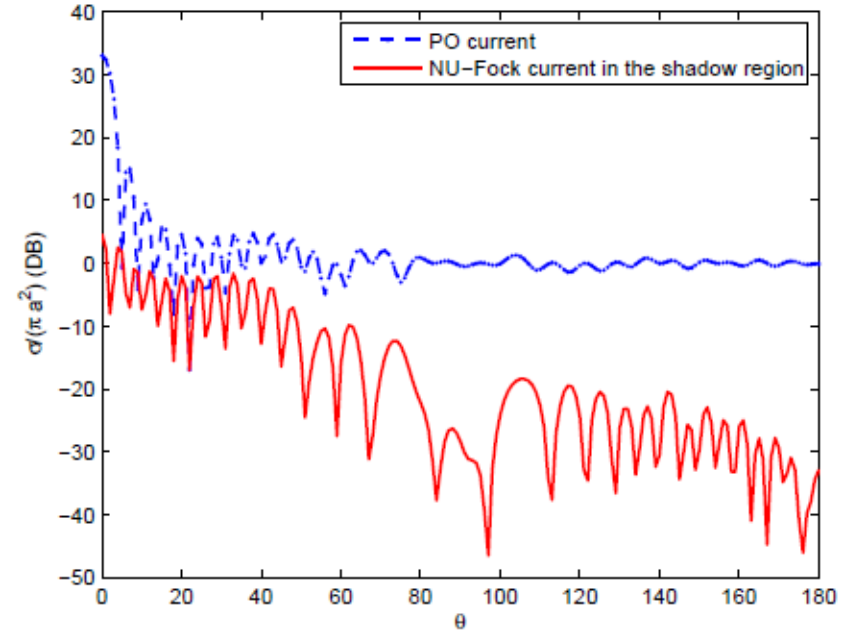
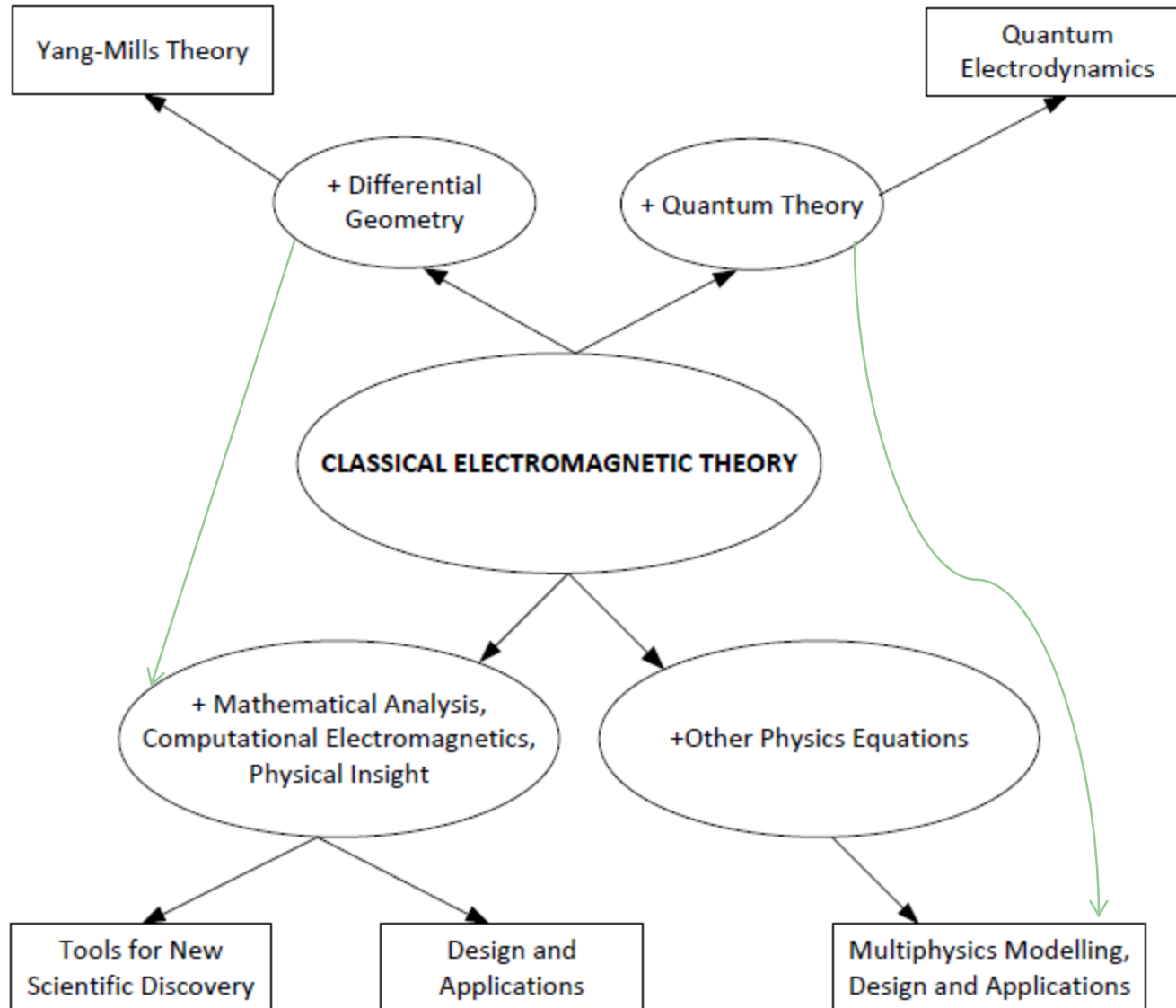


Fig. 10. Comparison of the contributions of the PO scattered fields and the wave fields from the NU-Fock current in the shadow region of the sphere, with $kR = 45$.

What's in Store for Us in the Future? Relational Diagram



Maxwell's Equations are Valid both in Classical Physics and Quantum Physics

Classical

$$\nabla \times \mathbf{H} = \mathbf{J} + \frac{\partial \mathbf{D}}{\partial t}$$

$$\nabla \times \mathbf{E} = -\frac{\partial \mathbf{B}}{\partial t}$$

$$\nabla \cdot \mathbf{D} = \rho$$

$$\nabla \cdot \mathbf{B} = 0$$



Quantum

$$\nabla \times \hat{\mathbf{H}} = \hat{\mathbf{J}} + \frac{\partial \hat{\mathbf{D}}}{\partial t}$$

$$\nabla \times \hat{\mathbf{E}} = -\frac{\partial \hat{\mathbf{B}}}{\partial t}$$

$$\nabla \cdot \hat{\mathbf{D}} = \hat{\rho}$$

$$\nabla \cdot \hat{\mathbf{B}} = 0$$

Mandel and Wolf: Quantum Optics

QED validated to 1 part in a trillion

Electromagnetics and Geometry

- Differential forms, Cartan, Deschamps, Desbrun;
- DeRham complex;
- Whitney forms;
- Yang-Mills theory.

$$d_D F = 0$$
$$*d_D * F = J.$$

Why is EM theory gauge invariant?

Why does EM theory inspire Yang-Mills theory?

Why does Yee algorithm work so well?

Why do some finite element method/MoM not converge or have poor accuracy?

Why is Chen-Wilton, Buffa-Christensen basis needed?

Why divergence conforming basis?

Why curl conforming basis?

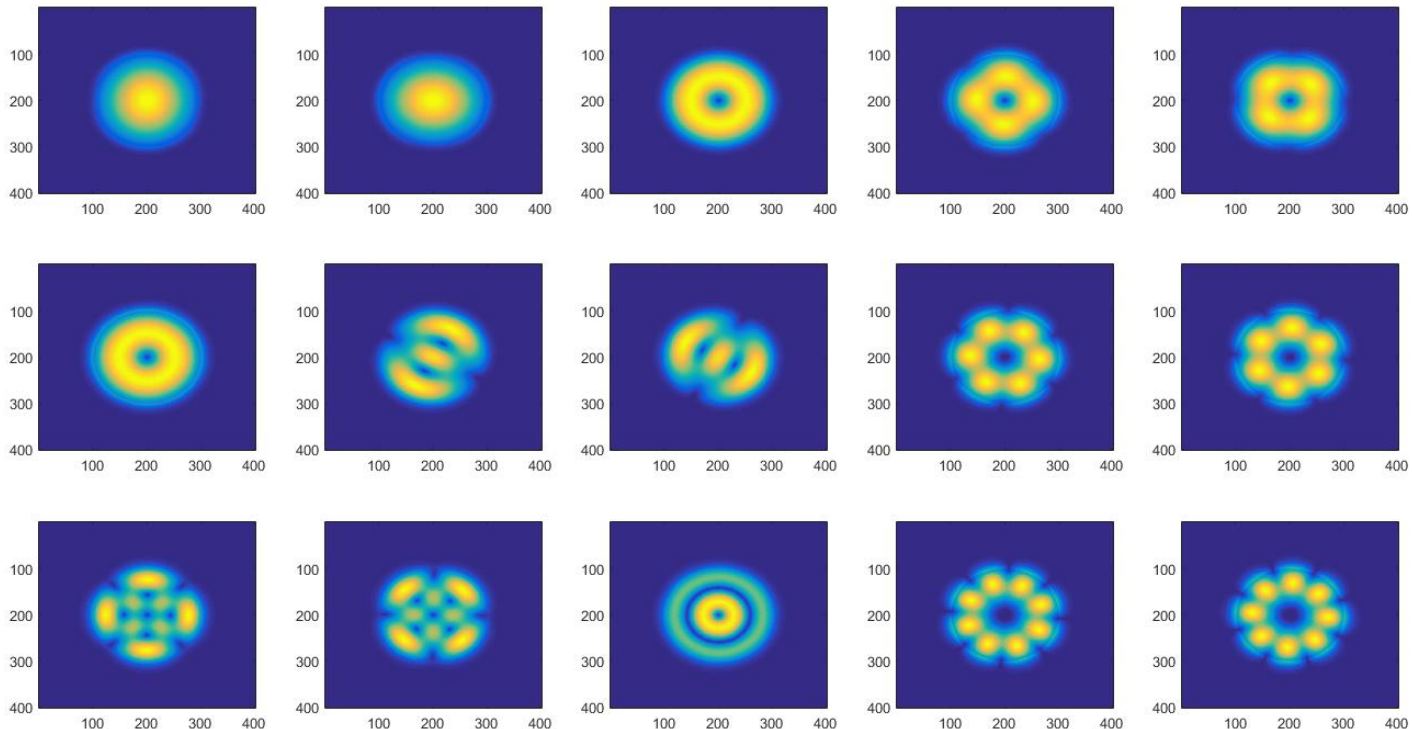
W. C. Chew, J. Applied Physics, vol. 75, no. 10, pp. 4843-4850, May 1994.

Differential Forms for CEM (Shu Chen)

- Discrete exterior calculus (Desbrun 2008);
 - **Inhomogeneous optical waveguides (optical fiber)**

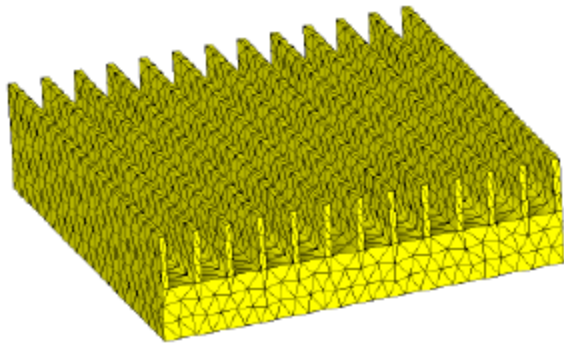
$$\bar{\mu}_s \cdot \hat{z} \times \nabla_s \times \mu_{zz}^{-1} \nabla_s \times \mathbf{E}_s - \hat{z} \times \nabla_s \epsilon_{zz}^{-1} \nabla_s \cdot \bar{\epsilon}_s \cdot \mathbf{E}_s - \omega^2 \bar{\mu}_s \cdot \hat{z} \times \bar{\epsilon}_s \cdot \mathbf{E}_s = -k_z^2 \hat{z} \times \mathbf{E}_s$$

$$\left\{ (\star_{\mu_s}^1)^{-1} (d^1)^t \star_{\mu_z}^2 d^1 + d^0 (\star_{\epsilon_z}^0)^{-1} (d^0)^t \star_{\epsilon_s}^1 - \omega^2 (\star_{\mu_s}^1)^{-1} \star_{\epsilon_s}^1 \right\} E_s = -k_z^2 E_s$$

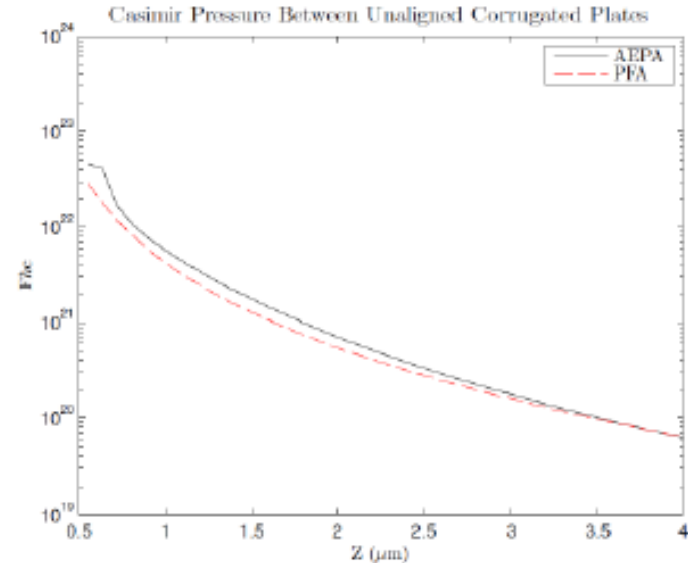


Casimir Force and CEM—Quantum (with J. Xiong, P.R. Atkins, Z.H. Ma, Q. Dai, W. Sha)

- **Casimir force calculation of two corrugated surfaces**



Geometrical mesh of one of the two corrugated surfaces



Casimir force between two corrugated surfaces using EPA vs PFA (proximity force approximation)

Maxwell-Schrödinger System (C. Ryu)

Electromagnetics Equations*

$$\nabla \cdot \epsilon \nabla \Phi - \epsilon^2 \mu \frac{\partial^2}{\partial t^2} \Phi = -\rho_q$$

$$-\nabla \times \mu^{-1} \nabla \times \mathbf{A} - \epsilon \frac{\partial^2}{\partial t^2} \mathbf{A} + \epsilon \nabla \epsilon^{-2} \mu^{-1} \nabla \cdot \epsilon \mathbf{A} = -\mathbf{J}_q$$

$$\nabla \cdot \mathbf{J}_q + \frac{\partial \rho_q}{\partial t} = 0$$

- Stable in low frequency \rightarrow Suitable for this system.
- Avoids the extra step of calculating the potentials from the fields.

Schrödinger Equation

$$i\hbar \frac{\partial}{\partial t} \psi = \frac{1}{2m^*} \left[\left(\frac{\hbar}{i} \nabla - q\mathbf{A} \right)^2 + \Phi + V \right] \psi$$

- Charged particle under an EM radiation.

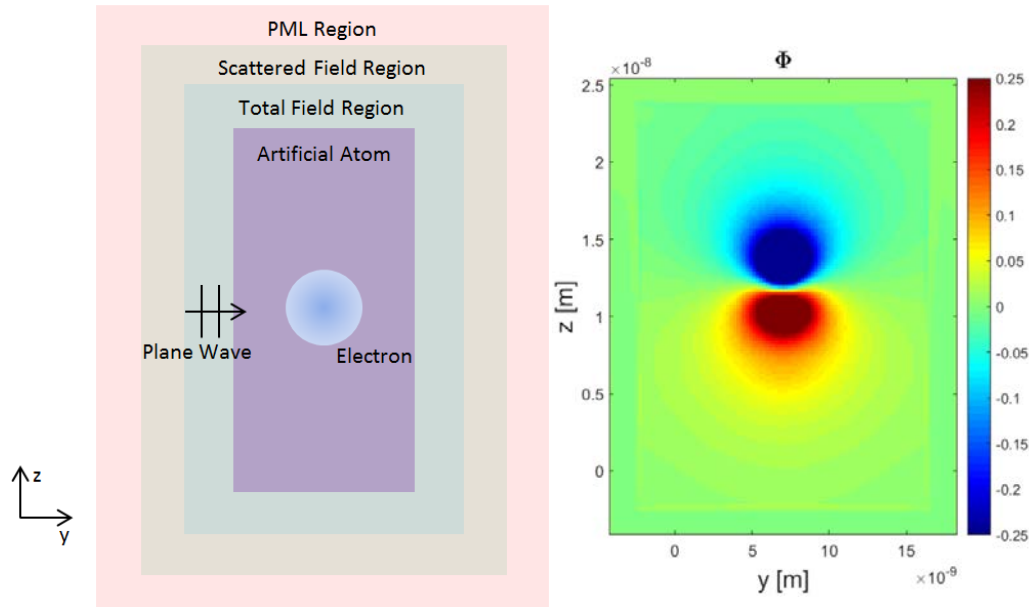
Particle Current

$$\mathbf{J}_q = \frac{q}{2} \left\{ \left[\frac{\hat{p} - q\mathbf{A}}{m^*} \psi \right]^* \psi + \psi^* \left[\frac{\hat{p} - q\mathbf{A}}{m^*} \right] \psi \right\}$$

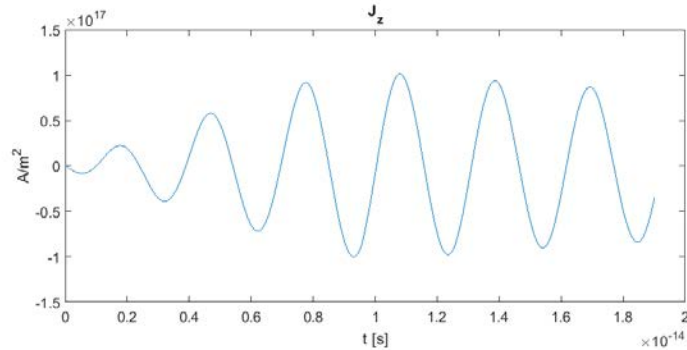
- Movement of the particle generates an electric current term.

S. Ohnuki of Japan
T. Rozzi of Italy

Simulation of an Artificial Atom (C. Ryu)

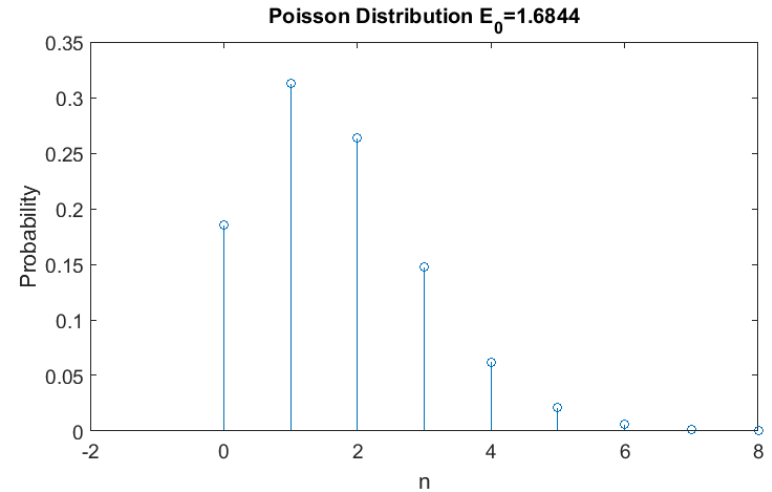


The artificial atom **forms a dipole** when excited by a plane wave. It generates an electric current density as shown below.

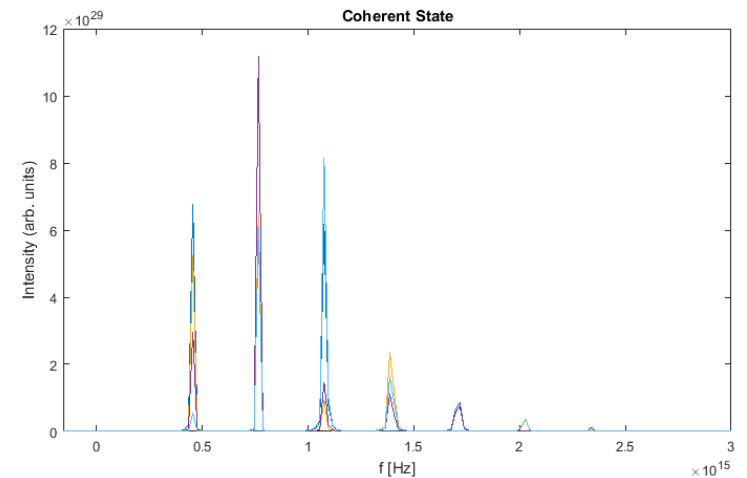


Simulation of a Coherent State

Expected State Distribution



Simulated State Distribution



Conclusions

- Give the historical background and EM physics of optics and electromagnetics;
- Review some of our past and present works;
- Much physical insight and mathematical finesse are needed to solve EM problems;
- Computational electromagnetics (CEM) will become increasingly more important in nano-optics, quantum optics, and quantum information, and imaging;
- Modern forms of electromagnetics (quantum and geometry) will inspire more computational electromagnetic problems;
- Experiments have always propelled new knowledge;
- Important that CEM/experiment researchers work together.

Thank you for your attention!

Mathematics is the Mother of Science,

Science is the Father of Technology,

Technology is the Gift of God!

Are Maxwell's Equations the Gift of God?

The University of Illinois at Urbana-Champaign - Oasis in a Corn Field

